SOME DOPPLER SHIFT LIFETIMES IN P^{30}

by

André Lachaîne

Submitted in partial fulfillment of the

requirements for the degree of Master of Science

Department of Physics
Faculty of Science and Engineering
University of Ottawa
Ottawa, Ontario
April 1970

A ma femme,

CAROLE

ABSTRACT

The Doppler shift attenuation method has been used to study the lifetimes of some levels in P^{30}. These levels were populated by resonances at proton energies of 1505, 1643, 1686, 1773 and 1775 Kev in the $Si^{29}(p,\gamma)P^{30}$ reaction.

Lifetimes of 360^{+3100}_{-220} fs, 85^{+45}_{-30} fs, 38 ± 6 fs, 2000^{+3000}_{-800}, and 215^{+105}_{-65} fs were found for the levels at excitation energies of 1.974, 2.936, 4.142, 4.231 and 4.624 Mev respectively. Upper limits of $\leq$14 fs, $\leq$15 fs, and $\leq$47 fs were set on the lifetimes of the 3.020, 4.182 and 4.501 Mev levels respectively, while a lower limit of $\geq$ 1100 fs was set on the lifetime of the 0.709 Mev level.

ACKNOWLEDGEMENTS

I wish to thank my thesis director, Dr. B. Hird, for his encouragement and counsel in the accomplishment of this project.

I am endebted to Dr. A. L. Carter for his work on the stabilization of the Ge(Li) counter system.

I wish to express my gratitude to Dr. L. Pai and Mr. R. Gauthier for the friendship and advice with which they provided me throughout the experiments.

Also, I wish to thank Mr. G. Drzewicki for his assistance in drawing the figures and Mr. L. Culomovic for his aid in writing the computer programs.

Finally, I am endebted to Miss D. Dubé for typing this thesis.

This research was supported by the Province of Ontario and by the National Research Council of Canada.

TABLE OF CONTENTS

LIST OF FIGURES

LIST OF TABLES

CHAPTER 1

INTRODUCTION

1.1 Review of Some $Si^{29}(p,\gamma)P^{30}$ Properties

At the time when these $Si^{29}(p,\gamma)P^{30}$ experiments were undertaken, very little was known on the lifetimes of excited states in P^{30}. Kennedy et al.[1] had measured the lifetimes of the first two excited levels via the $Al^{27}(\alpha,n)P^{30}$ reaction and had found them to be τ (0.680 Mev) = (1.55±.3) $X10^{-13}$sec and τ (0.709 Mev)$\geq 3X10^{-12}$sec, but the lifetimes of the other levels were unknown.

In 1963, Moore[2] studied the decay schemes of ten resonances in the range Ep = 1100 - 1800 Kev. Similar work has been done by Val'ter et al[3] on the Ep = 1308 Kev resonance and by Phelps et al[4] on five resonances in the range Ep = 1470 - 2120 Kev. Endt and Van der Leun[5], who reviewed the properties of the P^{30} nucleus, gave a comprehensive view of the decay schemes of the resonances up to Ep = 1772 Kev.

By far the most detailed investigation was done by Harris et al[6], who studied the Ep = 730, 917, 1302, 1470, 1505, 1686 and 1748 Kev resonances, giving a clearer picture of their decay schemes and branching ratios. Vermette et al[7] used the $Si^{28}(He^3,p)P^{30}$ reaction to study decay schemes of bound levels in P^{30}.

The experimental work described in this thesis is concerned with the determination of the lifetimes of levels in P^{30}, using the Doppler shift attenuation method. Recently, it was learned that Harris et al[8]

had determined the lifetimes of several levels in P^{30}, and had made some clarifications in the decay schemes of some resonances. Their results, along with those of Kennedy et al. are tabulated in table 1.

Three levels whose lifetimes have not been determined by Harris et al. were investigated (Ex = 3.020, 4.182, 4.501 Mev) and limits were set on their lifetimes. Also, other levels which had been investigated by Harris et al. were studied, some via resonances different from those used by them to determine lifetimes.

The lifetimes of the nuclear levels measured in this work were obtained by means of the Doppler shift attenuation method (Devons et al[9]), which, for the study of proton capture reactions at these bombarding energies, was made possible by the high resolution of the Ge(Li) gamma-ray spectrometer.

1.2 The Resonances Used to Determine the Lifetimes.

The resonances used to populate the P^{30} levels were at proton energies of Ep = 1505, 1643, 1686, 1773 and 1775 Kev. The decay schemes which were used in interpreting the gamma-ray spectra are those given by Harris et al.[6,8] Table 2 summarizes some of the properties of these resonances.

A. The Ep = 1505 Kev Resonance

This resonance, which Harris [8] has found is actually a doublet, with a weak member at Ep = 1502 Kev was studied to determine the scope of the Ge(Li) gamma-ray spectrometer in studying radiative capture reactions,

TABLE I

Known Lifetimes of P^{30} Levels Previous to this Work. *

E_x (Mev)	τ ($\times 10^{-15}$ sec.)
0.678	155 ± 30
0.709	≥ 3000
1.453	≥ 240
1.974	≥ 240
2.536	92 ± 21
2.723	96 ± 15
2.939	37 ± 5
4.142	58 ± 14
4.231	≥ 1200
4.421	64 ± 8
4.468	≤ 33
4.624	260 ± 60
4.921	≥ 800
4.945	47 ± 20

* Refs.1 and 8.

TABLE II

The Resonances Studied in the Present Work. *

E_p (Kev)	E_x (Mev)	J^π	Γ (Kev)	$S=(2J+1)\Gamma_\gamma \Gamma_p / \Gamma$ (ev)
1505	7.052	4^-	≤ 3	5.0 ± 1.0
1643	7.185	1^-	17.2 ± 2	14 ± 3
1686	7.227	2^-	$5.9 \pm .7$	11 ± 2
1773	7.311		≤ 1.5	$0.87 \pm .17$
1775	7.313	(3)	≤ 1.5	1.1 ± 0.2

* Taken from Harris, et al. Ref.8.

to develop the techniques of high resolution spectroscopy, and to establish an energy scale and thus calibrate the spectrometer for further experiments. Its decay scheme is presented in figure 1. This resonance was used to determine the lifetime of the 4.23 and 4.62 Mev levels.

B. The Ep = 1643 Kev Resonance

The decay scheme of this resonance (cf Figure 2) is taken from Endt and Van der Leun[5] and Harris[8]. It was used to set limits on the lifetimes of the 3.02 Mev and 0.709 Mev levels.

C. The Ep = 1686 Kev Resonance

This strong resonance was studied to determine the lifetime of the 4.14 Mev level. It was also used to obtain the Ep = 1643 Kev resonance, since it is only 43 Kev away from the latter. Its decay scheme, due to Harris [6,8], is shown in Figure 3.

D. The Ep = 1774 Kev Resonance

This resonance was shown by Harris[8] to be a doublet at Ep = 1773 Kev and Ep = 1775 Kev. In our experiments, since the beam energy spread is about 5 kev at 1 Mev (Gauthier[10]), both resonances were excited simultaneously. The Ep = 1773 Kev resonance populated the 1.97, 4.18 and 4.50 Mev levels and had not been used by Harris to determine lifetimes. The Ep = 1775 Kev level populated the 2.94 Mev level and the 1.97 Mev level. Figures 4 and 5 show the decay schemes of both these resonances.

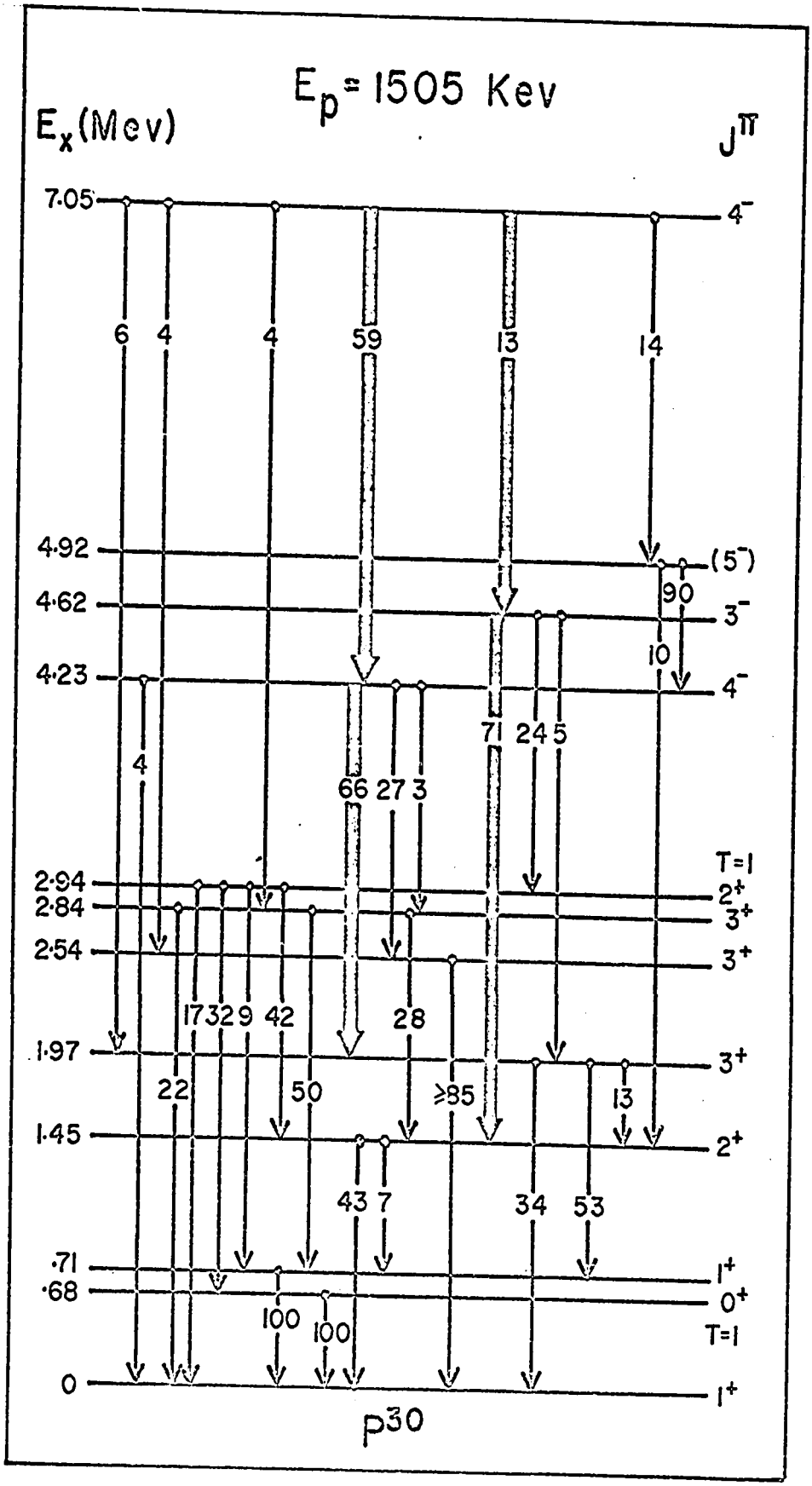
E_p = 1505 Kev
E_x(Mev)
J^π
7.05
4⁻
6
4
4
59
13
14
4.92
(5⁻)
90
4.62
3⁻
10
4.23
4⁻
71
24
5
4
66
27
3
T=1
2.94
2⁺
2.84
3⁺
2.54
3⁺
17
32
9
42
28
1.97
3⁺
22
50
≥85
13
1.45
2⁺
43
7
34
53
.71
1⁺
.68
0⁺
100
100
T=1
0
1⁺
p30

FIGURE 1

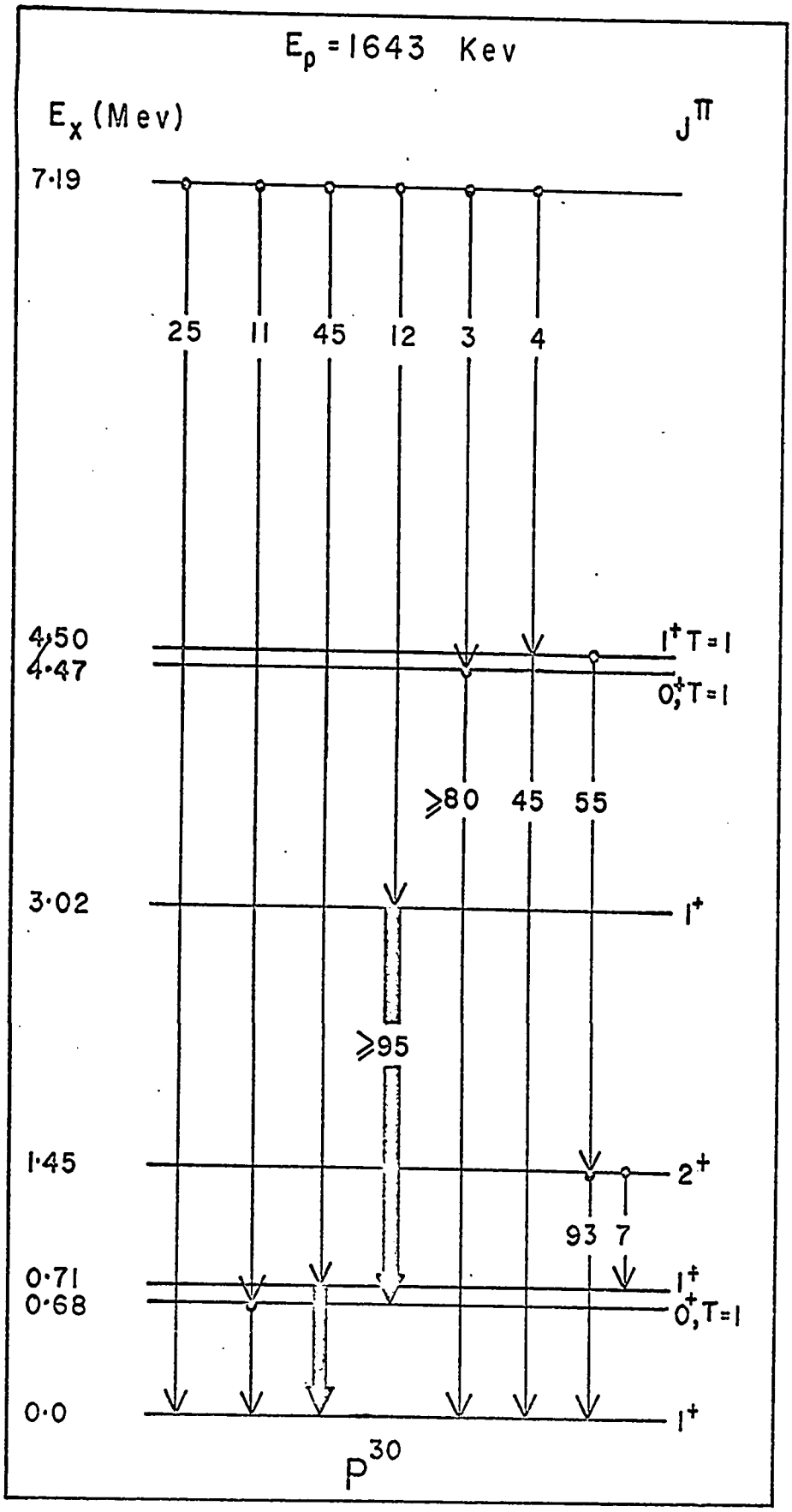
E_p = 1643 Kev
E_x (Mev)
J^π
7·19
25
11
45
12
3
4
4·50
4·47
1^+ T=1
0^+ T=1
≥80
45
55
3·02
1^+
≥95
1·45
2^+
93
7
0·71
0·68
1^+
0^+, T=1
0·0
1^+
P^{30}

FIGURE 2

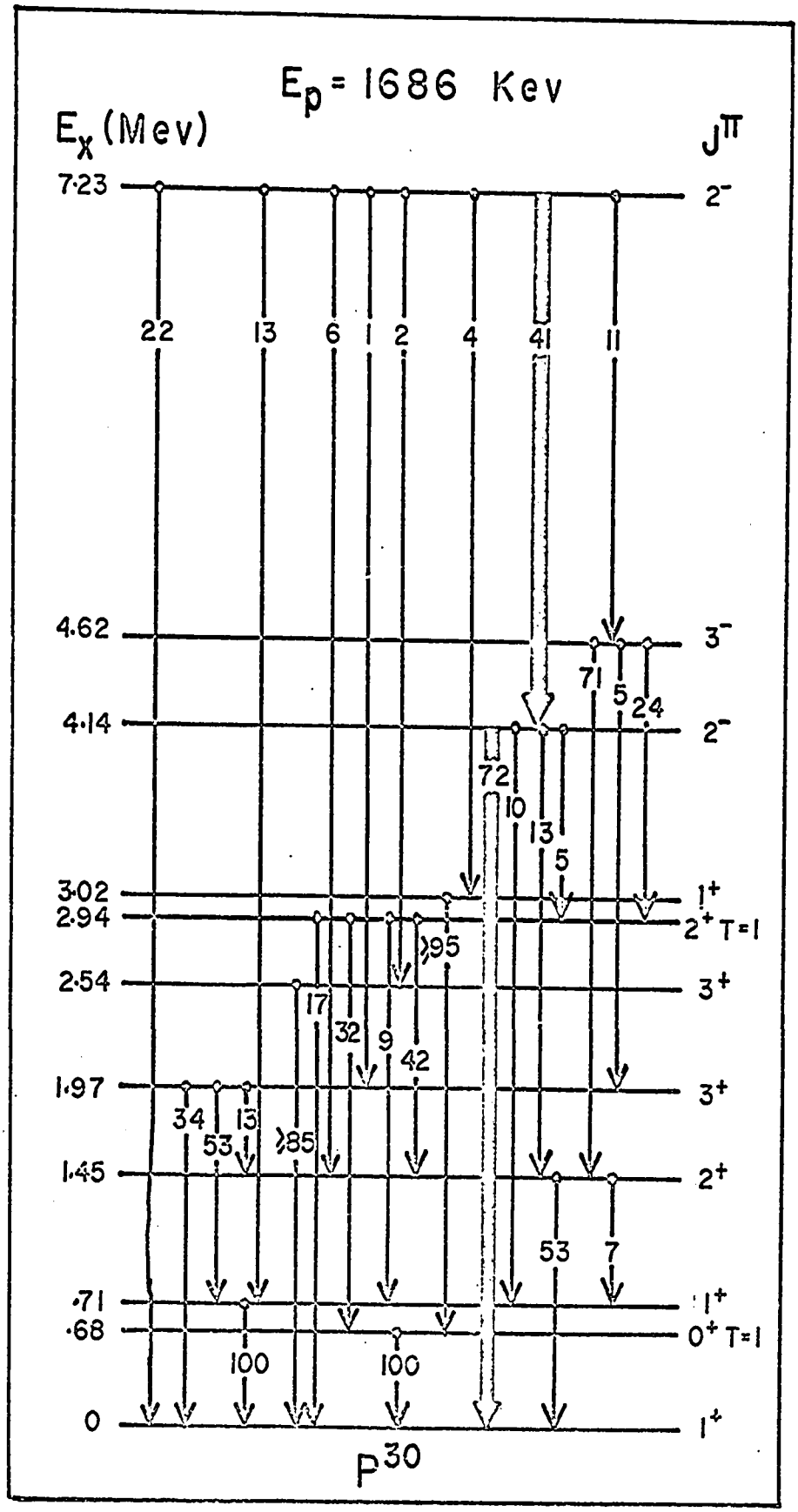
E_p = 1686 Kev
E_x (Mev)
J^π
7.23
2⁻
22
13
6
1
2
4
41
11
4.62
3⁻
71
5
24
4.14
2⁻
72
10
13
5
3.02
1⁺
2.94
2⁺ T=1
≥95
2.54
3⁺
17
32
9
42
1.97
3⁺
34
53
13
≥85
1.45
2⁺
53
7
.71
1⁺
.68
0⁺ T=1
100
100
0
1⁺
P30

FIGURE 3

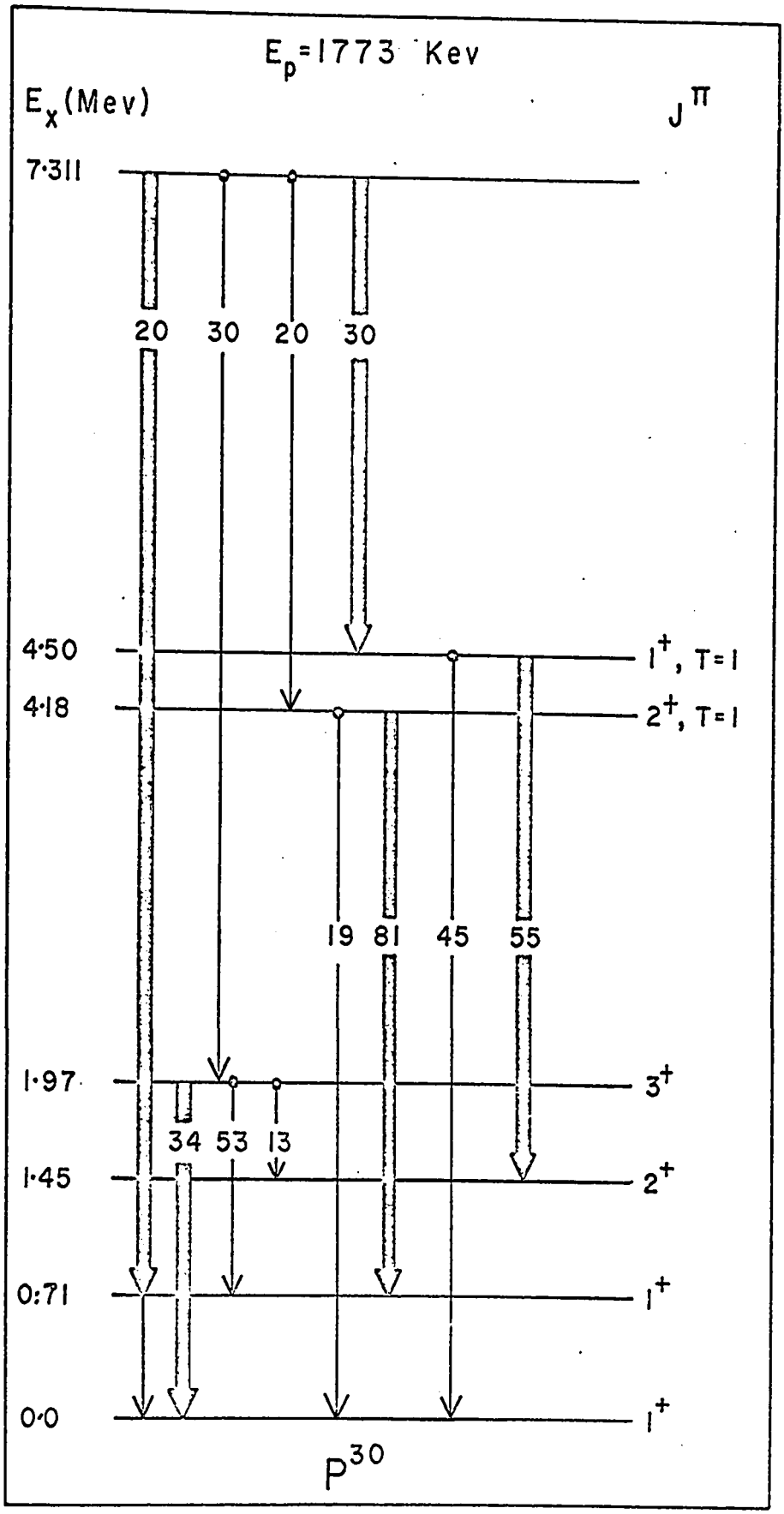
E_p=1773 Kev
E_x(Mev)
J^π
7·311
20
30
20
30
4·50
1^+, T=1
4·18
2^+, T=1
19
81
45
55
1·97
3^+
34
53
13
1·45
2^+
0·71
1^+
0·0
1^+
P^{30}

FIGURE 4.

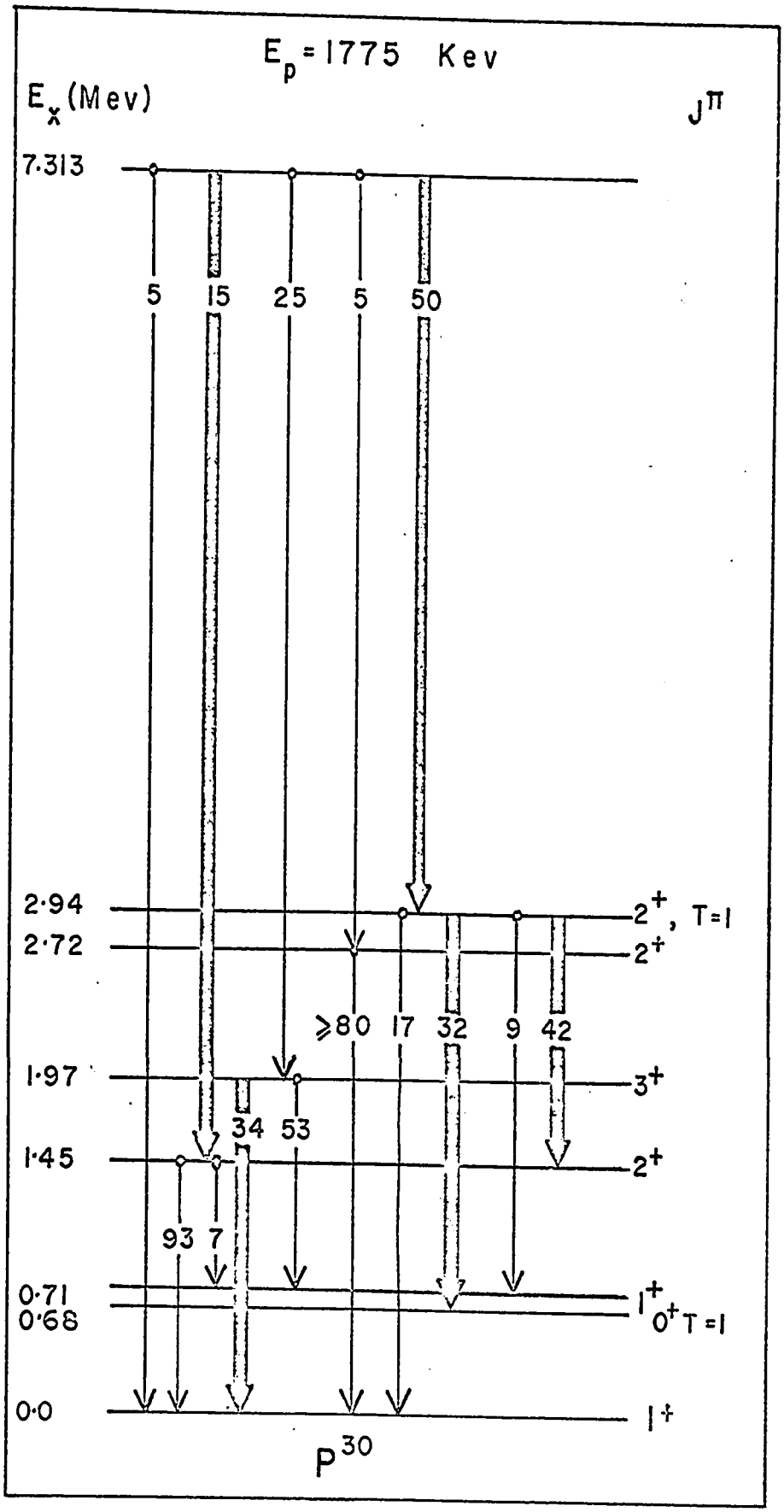
E_p = 1775 Kev
E_x (Mev)
J^π
7.313
5
15
25
5
50
2.94
2^+, T=1
2.72
2^+
≥80
17
32
9
42
1.97
3^+
34
53
1.45
2^+
93
7
0.71
1^+
0.68
0^+ T=1
0.0
1^+
P^{30}

FIGURE 5

CHAPTER 2

EXPERIMENTAL PROCEDURE

2.1 General

A. Detection of The Gamma-Rays.

The gamma-rays were detected by means of a 30 CC. ORTEC Lithium-drifted Germanium detector, whose resolution was measured to be 6 Kev for the 1.33 Mev Co^{60} line. Figure 6 shows a block diagram of the electronic circuitry used to detect and observe the gamma radiation. Spectra were stored in a 4096 channel PDP-9 computer, equipped with a digital stabilizer to minimize the gain drifts. The amplifier and ADC were kept in a temperature-controlled rack, where the temperature was observed to vary by at most $\pm.5\ c^{0}$ (cf Figure 7).

The spectrometer was first calibrated with a Co^{60} source ($E\gamma$ = 1.33 Mev) and a Na^{24} source ($E\gamma$ = 2.75 Mev). It was later recalibrated to cover a wider range of energy, by using known gamma-rays from the Ep = 1505 Kev resonance.

The linearity of the Ge(Li) system was determined with the aid of a sliding pulse generator of variable voltage, used to produce peaks at various channels in the computer. The voltage corresponding to each peak, and the peak centroid were determined, and, with the aid of a computer program, a graph of the deviation from linearity as a function of channel number was plotted (cf Figure 8). Also, the counting rate in the Ge(Li) spectrometer was kept below 250 counts/sec, since a counting

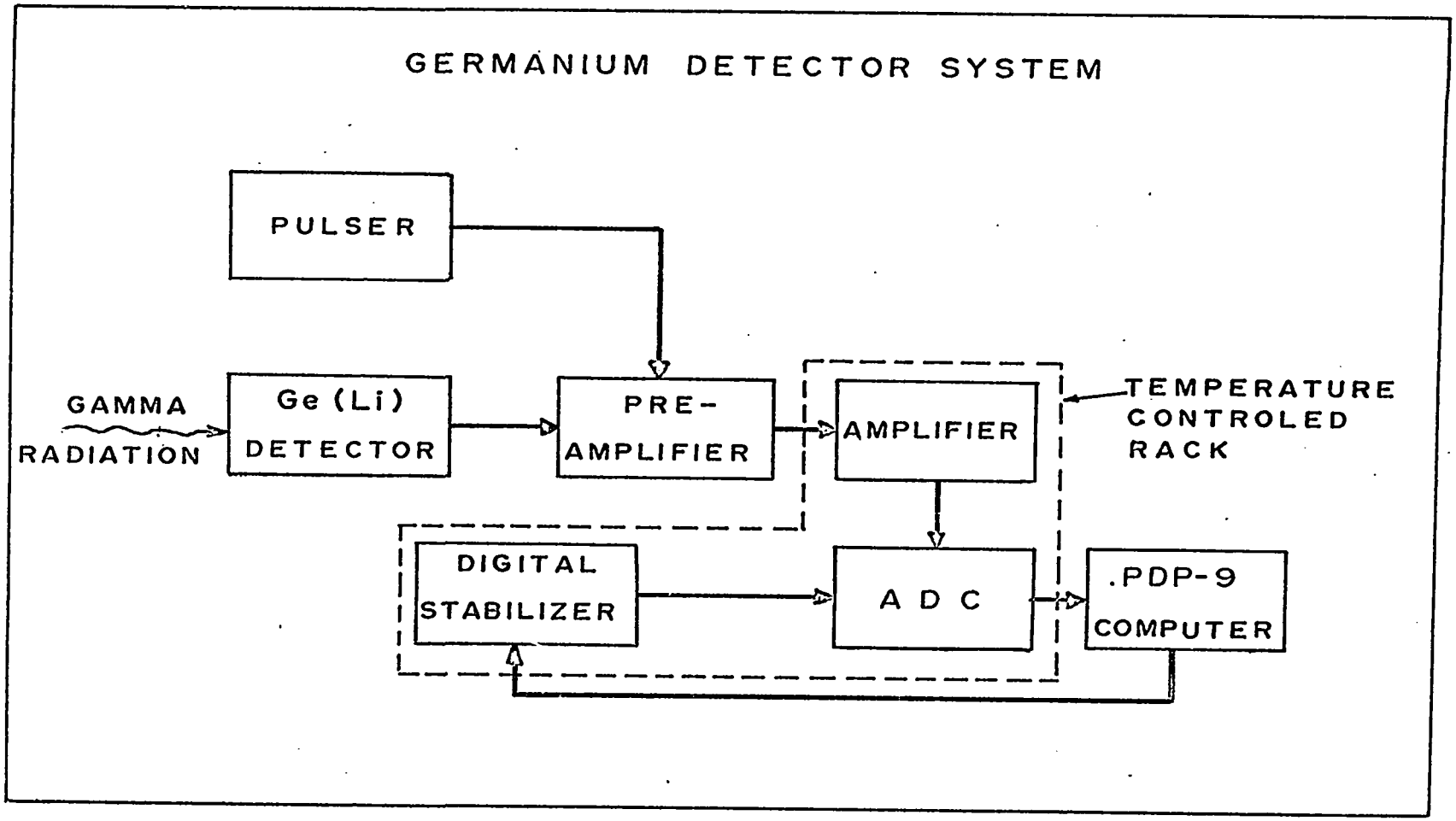
GERMANIUM DETECTOR SYSTEM
PULSER
GAMMA RADIATION
Ge (Li) DETECTOR
PRE-AMPLIFIER
AMPLIFIER
TEMPERATURE CONTROLED RACK
DIGITAL STABILIZER
A D C
.PDP-9 COMPUTER

FIGURE 6

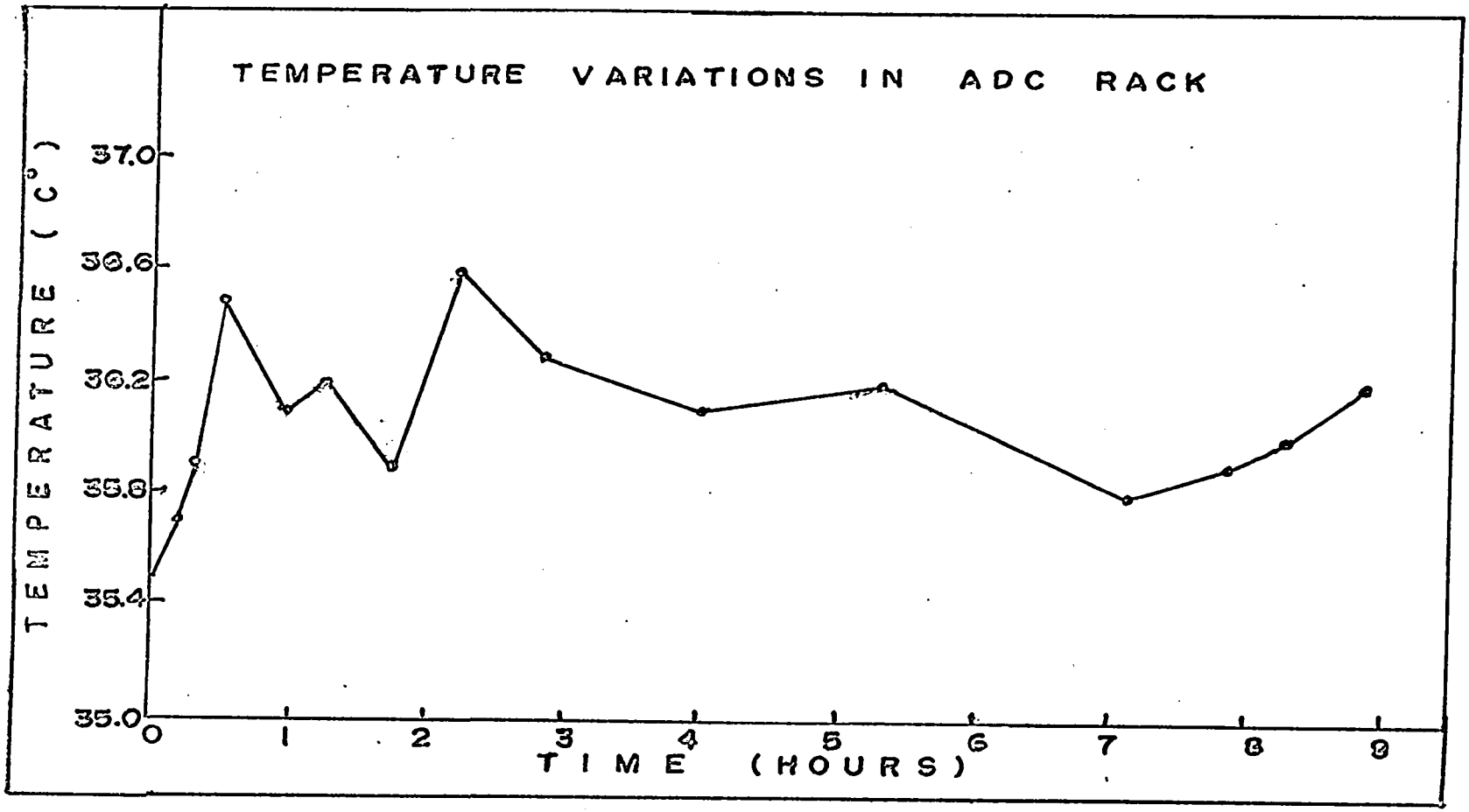
TEMPERATURE VARIATIONS IN ADC RACK
TEMPERATURE (C°)
37.0
36.6
36.2
35.8
35.4
35.0
0
1
2
3
4
5
6
7
8
9
TIME (HOURS)

FIGURE 7

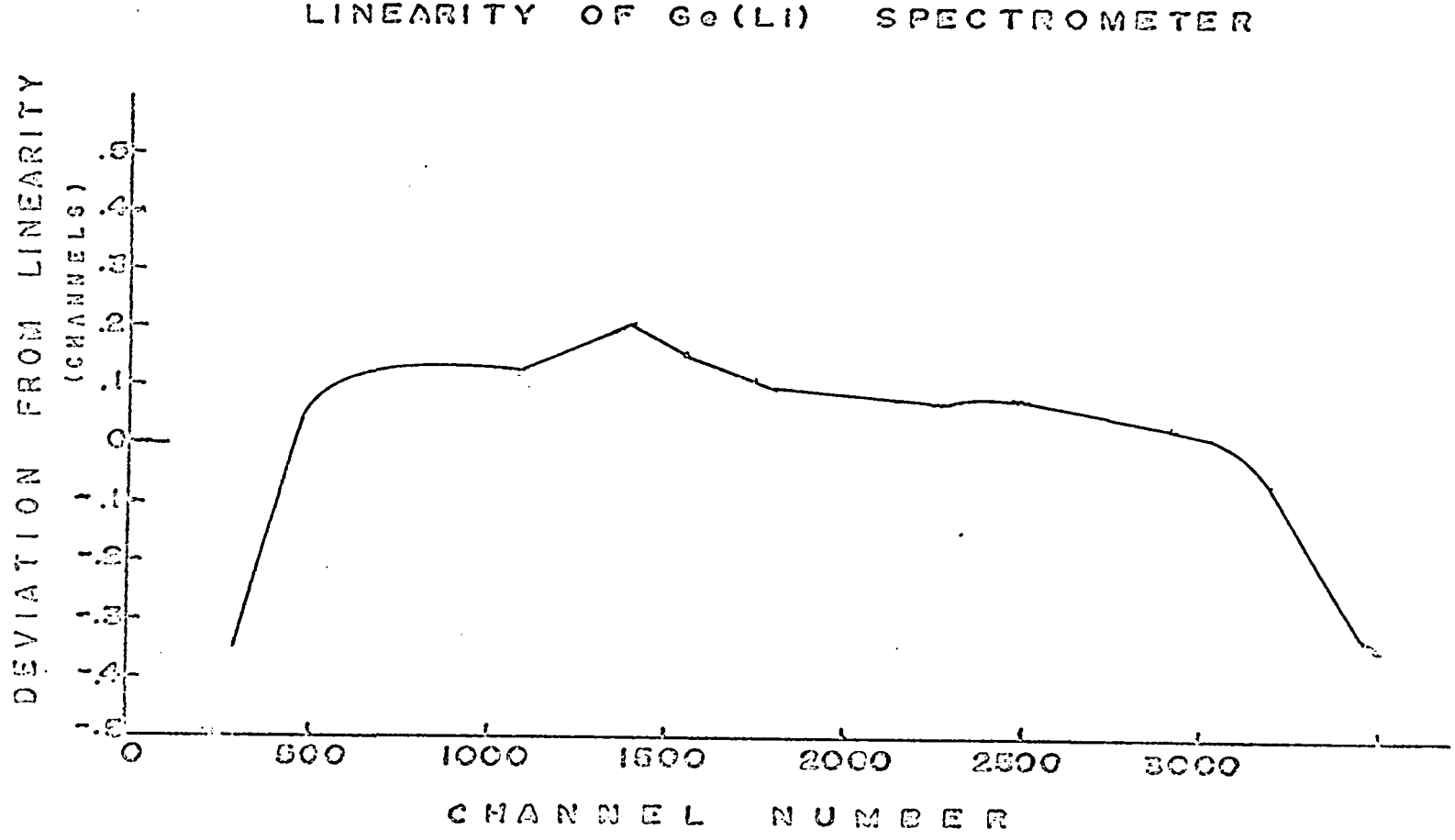
LINEARITY OF Ge(Li) SPECTROMETER
DEVIATION FROM LINEARITY
(CHANNELS)
.5
.4
.3
.2
.1
0
-.1
-.2
-.3
-.4
-.5
0
500
1000
1500
2000
2500
3000
CHANNEL NUMBER

FIGURE 6

rate higher than this was noticed to produce a change in the centroid of the pulser used to stabilize the system (cf Figure 9).

Spectra were accumulated at two angles, θ_1 and θ_2, for a given resonance, and the first moments of the various peaks were calculated with a computer program. The uncertainties in the centroids were taken to be the standard deviation in the first moments of the peaks.

i.e. $$\Delta\bar{x} = \frac{1}{N}\sqrt{\sum_{k=1}^{n} (\bar{x} - x_k)^2 (N_{Tk} + N_{Bk})}$$

where N = total number of counts in the peak

N_{Tk} = total number of counts (including background in the k^{th} channel x_k.)

N_{Bk} = number of counts in the k^{th} channel due to background only

$\bar{x}$ = centroid of peak

The attenuation coefficient $$F = \frac{E(\theta_1) - E(\theta_2)}{(\Delta E)\ \text{F.D.S.}}$$

where $E(\theta)$ = energy of gamma-ray at angle θ

and

(ΔE) F.D.S. = calculated full Doppler shift energy,

was calculated, along with its uncertainty, for each gamma-ray, and, with the aid of a computer program, the lifetimes of the levels were determined.

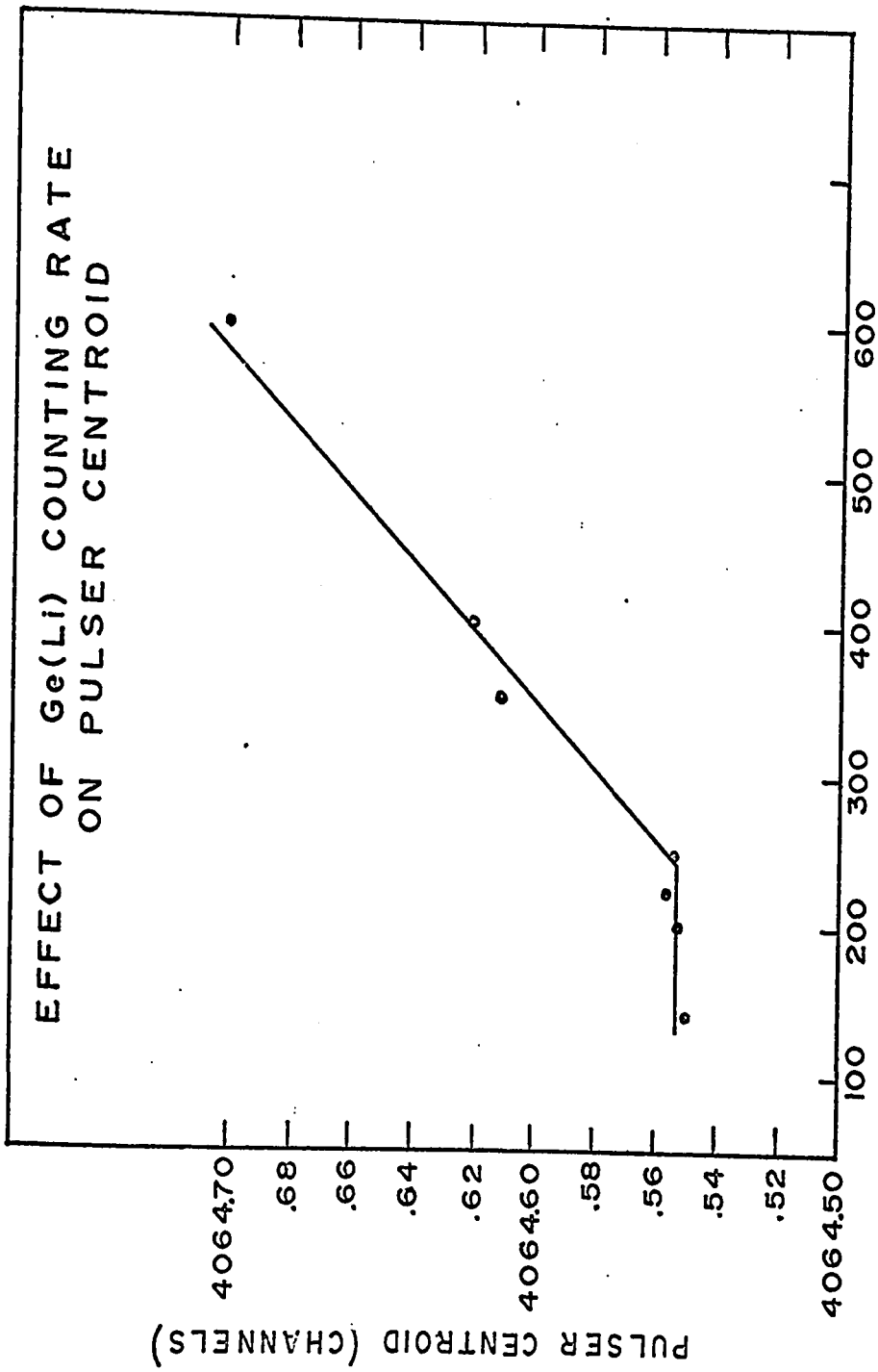
EFFECT OF Ge(Li) COUNTING RATE
ON PULSER CENTROID
PULSER CENTROID (CHANNELS)
4064.70
.68
.66
.64
.62
4064.60
.58
.56
.54
.52
4064.50
100
200
300
400
500
600
COUNTING RATE (COUNTS/SEC.)

FIGURE 9

B. Proton Energy and Target Considerations.

The proton capture experiments were performed at the University of Ottawa using the 3 MV Dynamitron accelerator, whose beam energy spread was measured to be 5 Kev at 1Mev (Gauthier[10]).

The energy calibration of the proton beam was carried out using the Ep = 1380 Kev and the Ep = 1724 Kev resonances in $Al^{27}(p,\gamma)Si^{28}$, whose gamma-ray spectra yields, in the case of the former, a characteristic gamma-ray at 2.837 Mev, and in the case of the latter, characteristic gamma-rays of 2.524 Mev and 5.856 Mev. A current of about 7μA was used to populate the resonances, which were observed by noting the yield of gamma-rays as a function of digital voltmeter readings. The gamma-rays were detected by means of a NaI(Tl) detector whose output was monitored on a scaler (cf Figure 10 for block diagram of NaI(Tl) electronics). The detection of the characteristic gamma-rays in the Ge(Li) spectrum then confirmed that these resonances had been attained, and the corresponding digital voltmeter readings were noted. Later, resonances in $Si^{29}(p,\gamma)P^{30}$ were obtained by extrapolation of these readings (cf Figure 11 for yield curve of the $Si^{29}(p,\gamma)P^{30}$ resonances)

The targets, $Si^{29}O_2$ enriched to approximately 75% Si^{29}, were obtained from AERE, Harwell. The target backings were copper disks, onto which was electroplated .002" gold to minimize background, which increases greatly above 1.2 Mev.

The target chamber, located adjacent to a liquid nitrogen cold trap, was cylindrical in shape, and permitted direct water cooling of the

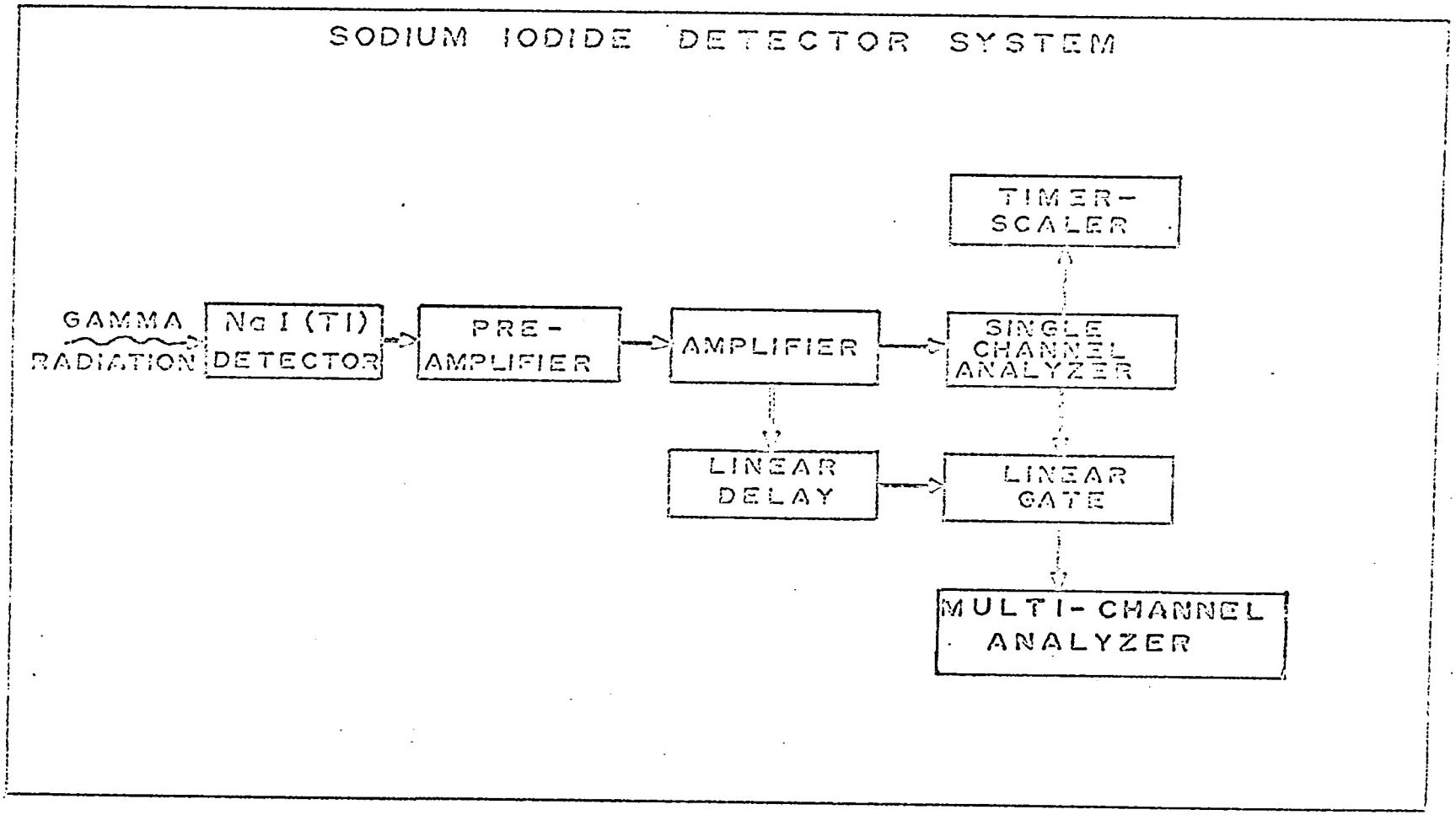
SODIUM IODIDE DETECTOR SYSTEM
GAMMA RADIATION
NaI (Tl) DETECTOR
PRE-AMPLIFIER
AMPLIFIER
TIMER-SCALER
SINGLE CHANNEL ANALYZER
LINEAR DELAY
LINEAR GATE
MULTI-CHANNEL ANALYZER

FIGURE 10

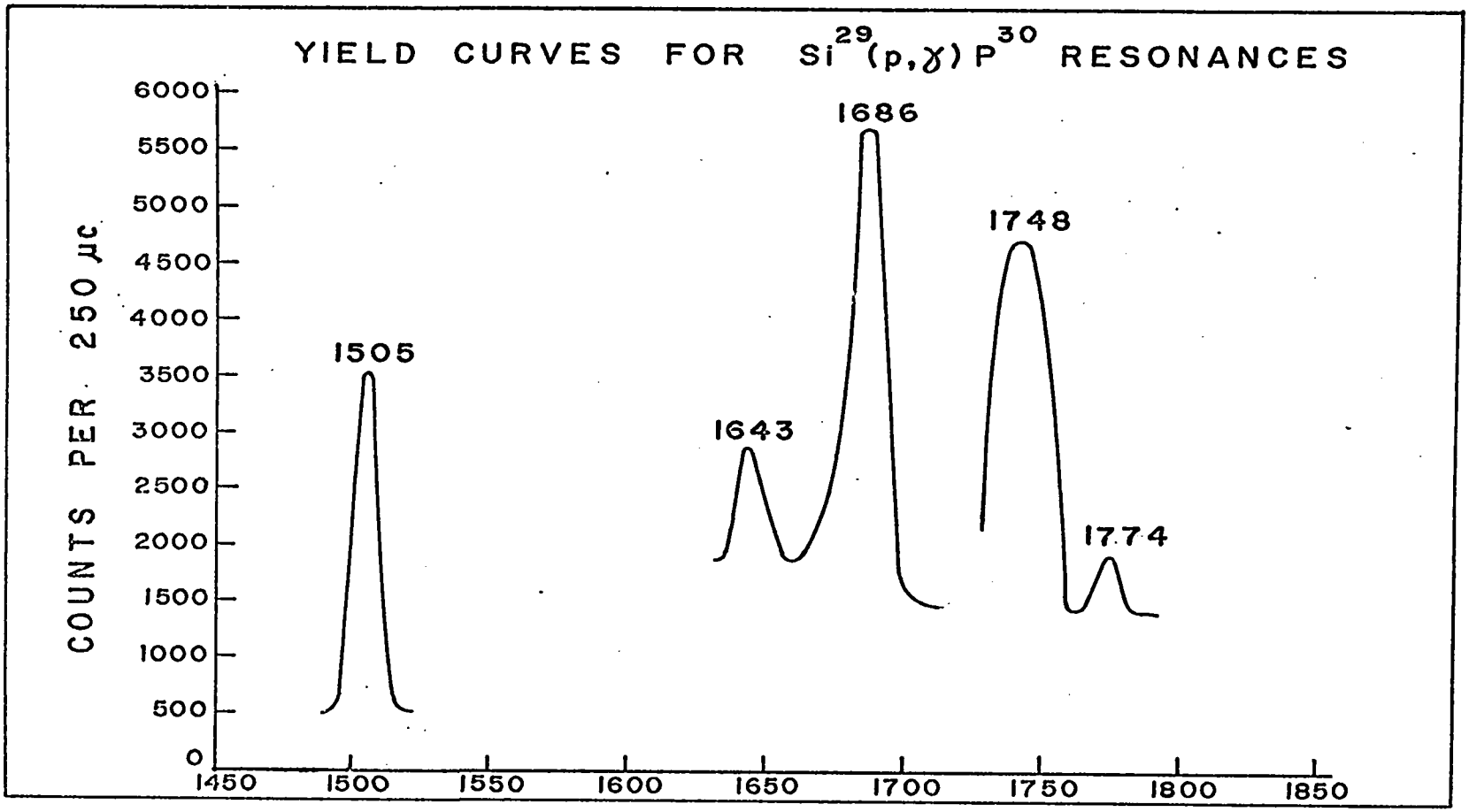
YIELD CURVES FOR Si29(p,γ)P30 RESONANCES
COUNTS PER 250 μc
6000
5500
5000
4500
4000
3500
3000
2500
2000
1500
1000
500
0
1505
1643
1686
1748
1774
1450
1500
1550
1600
1650
1700
1750
1800
1850
PROTON ENERGY (Kev)

FIGURE II

target (cf Figure 12).

The target thickness was approximately 70 $\mu g/cm^2$ which corresponds to .32 microns of $Si^{29}O_2$. Since the range of a 55 Kev P^{30} ion in $Si^{29}O_2$ is about .04 microns (Schiott[11]), most of the P^{30} ions were stopped in the target material itself, a fact which greatly simplifies the calculations since we deal with only one stopping medium.

C. Determination of the Resonances.

Five resonances were investigated in the reaction $Si^{29}(p,\gamma)P^{30}$, in which levels whose lifetimes were unknown were strongly populated. These resonances were the Ep = 1505 Kev, 1643 Kev, 1686 Kev, 1773 Kev and 1775 Kev. (cf Figure 11 for yield curve)

Spectra were first accumulated at 90^0, where there is no Doppler shift, to identify the resonances.

(i) The Ep = 1505 Kev Resonance

The 1505 Kev resonance was used to recalibrate the Ge(Li) spectrometer, since it gives characteristic gamma-rays at 5.078 Mev (R→1.974 Mev) and at 2.821 Mev (R→4.231 Mev). The lifetimes of the 4.231 Mev and 4.624 Mev levels in P^{30} were investigated via this resonance. Ge(Li) spectra were accumulated at 0^0 and at 90^0 in two series of measurements, (runs 1,2 and runs 13,15) lasting 1½ hours and 4 hours at each angle.

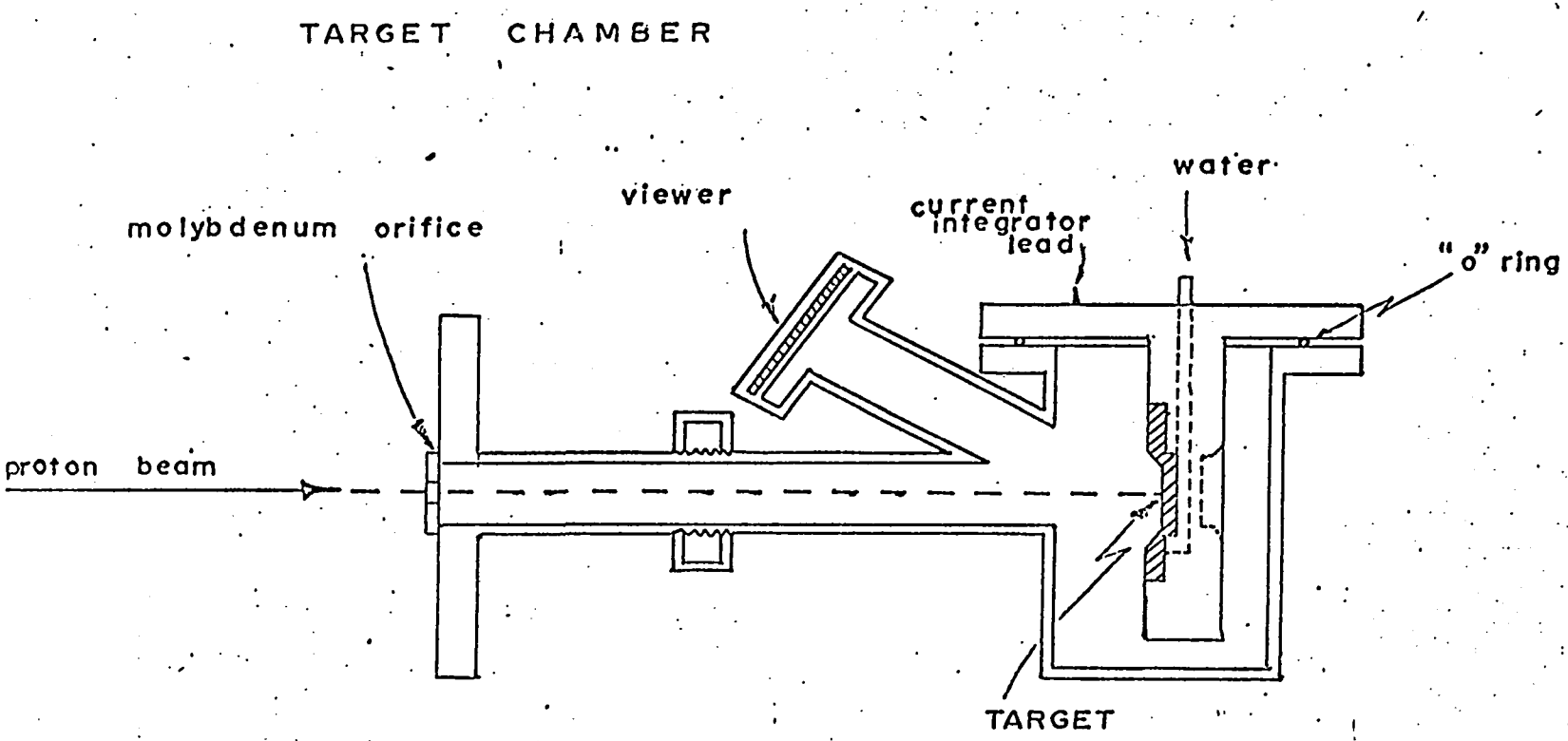
TARGET CHAMBER
molybdenum orifice
viewer
current integrator lead
water
"o" ring
proton beam
TARGET

FIGURE 12

(ii) The Ep = 1643 Kev Resonance

This resonance was measured at 0^0 and at 120^0 in two series of measurements at each angle (runs 9, 10, 11, 12), lasting 2 hours at each angle. The resonance was identified by a characteristic transition from the resonance level, 7.185 Mev, to the 3.020 Mev level, yielding a 4.165 Mev gamma-ray. The relevant energy levels that were populated were the 3.020 Mev and 0.709 Mev levels.

(iii) The Ep = 1686 Kev Resonance.

This resonance was identified by the presence of a strong 3.085 Mev gamma-ray, which results from the transition from the 7.227 Mev resonance level to the 4.142 Mev level. Ge(Li) detector spectra were accumulated at 0^0 and at 120^0, first for 1½ hours at each angle (runs 4, 5), then for 2 hours at each angle (runs 7, 8). This permitted the Doppler shift of the 4.142 Mev level to be measured.

(iv) The Ep = 1773 - 1775 Kev Doublet

This doublet populated the 1.974, 2.939, 4.182 and 4.501 Mev levels in P^{30}. Since the beam energy spread of the Dynamitron is about 5 Kev at 1 Mev, the resonances were not resolved.

The characteristic gamma-rays which permitted identification of the resonances were of energy 2.810 Mev and 6.602 Mev (corresponding to the 7.311→4.501 Mev and 7.311→.709 Mev transitions respectively) in the case of the 1773 Kev resonance, and 4.377 Mev (7.313→2.936 Mev) in the case of the 1775 Kev resonance. Germanium detector spectra were taken at 0^0 and at 90^0, for 4 hours at each angle.

2.2 The Stability of the Germanium Detector System.

Special attention was given to stabilize the Ge(Li) spectrometer, since good stability is crucial in Doppler shift measurements, particularly in (p,γ) reactions where the recoil energies are small. The stabilization of the gain of the detection system was accomplished by means of a Northern Scientific NS-404 Dual Digital Stabilizer (cf Figure 6).

A 60 cycle/sec pulse generator introduces a fixed charge into the preamplifier. This produces a reference voltage pulse which is amplified and stored in the top third of the memory of the PDP-9 computer. A digital window is then set up using the stabilizer front panel controls so that the center of this window corresponds to the center of the reference peak as observed in the stored spectrum. Also, the digital window width is adjusted so that only the reference peak is encompassed by the window.

With the system in operation, the number of counts in the upper half of the window will be equal to the number of counts in the lower half of the window. However, the instantaneous gain of the system changes with every count that falls within the window. Every time a count falls in the upper half of the window, the conversion gain is lowered slightly.

The net result is that, if there are no drifts in the system, the average conversion gain will be constant, while the instantaneous gain changes with every count that falls inside the window. A drift in gain anywhere in the system will upset the statistical equality in the number of counts in the two halves of the window, and the conversion gain will be changed, depending on which way the gain drifts.

It was found that for the stabilizer system to function properly, the gamma-ray counting rate had to be kept below 250 counts/sec, otherwise an asymmetry in the pulser peak was introduced, and the centroid of the peak moved. Below 250 c/s, no such asymmetry was observed. Figure 9 shows the change in centroid of the pulser peak as a function of gamma-ray counting rate.

Also, the amplifier and the ADC were kept in a temperature controlled rack. The temperature was recorded every hour and it appears that it was constant to within $\pm.5c^{0}$. (Figure 7)

Radioactive sources, such as Co^{60} & ThC" and known gamma-rays from the resonances were used to detect any gain drifts, and to obtain the energy dispersion (1.645 Kev/channel). The stability check was done in three ways: Firstly, before and after every run at a given angle, the centroids of the 1.17 and 1.33 Mev Co^{60} lines, and that of the 2.61 ThC" line were noted. Also, in some spectra, the Co^{60} lines were included. Secondly, in each spectrum there were certain gamma-rays which are known to have a full Doppler shift (i.e. gamma-rays decaying from the very short-lived resonance level); therefore a comparison could be made between the shift in the centroids of these peaks at the two angles and the known full Doppler shift. Thirdly, most resonances were done at two angles at least twice, therefore any drift in the centroid of a gamma-ray at a given angle during the elapsed time could be detected.

As a result of these checks, it was found that the system was stable to 0.5 channels over a period of 78 hours, and only one correction was applied, when there was a sudden change of .5 channels at 3 Mev, which occurred near the time between the 0^{0} and 120^{0} runs at the Ep = 1686 Kev resonance.

The stability of the system is demonstrated in figure 13, where the centroids of various γ-rays are plotted as a function of time. It should be noted that this graph displays the long term stability of the system, and that for short term stability checks between two runs, gamma-rays given off by the resonance (either fully Doppler shifted or unshifted) were used.

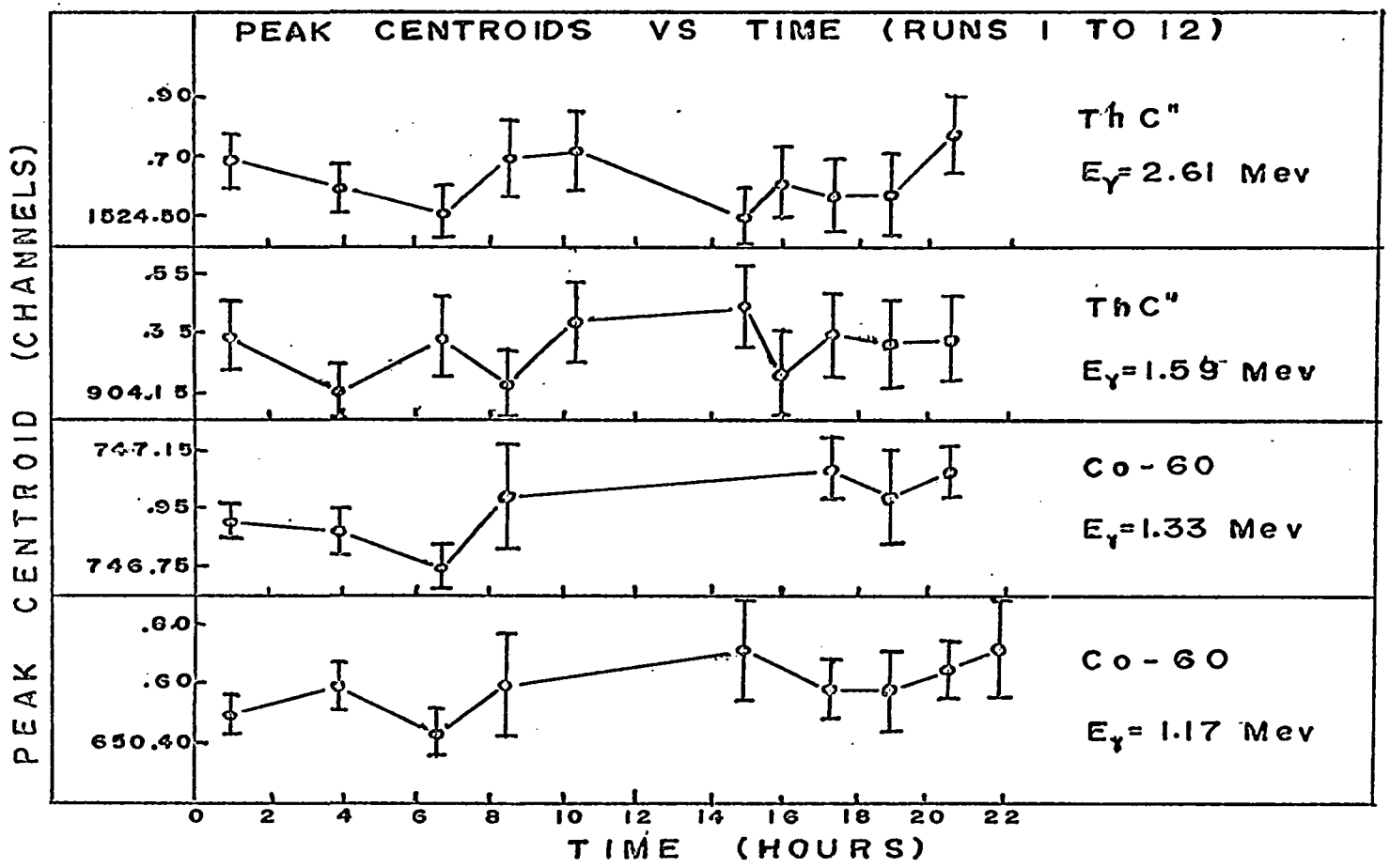
PEAK CENTROIDS VS TIME (RUNS 1 TO 12)
PEAK CENTROID (CHANNELS)
.90
.70
1524.50
ThC"
Eγ= 2.61 Mev
.55
.35
904.15
ThC"
Eγ= 1.59 Mev
747.15
.95
746.75
Co-60
Eγ= 1.33 Mev
.60
.60
650.40
Co-60
Eγ= 1.17 Mev
0 2 4 6 8 10 12 14 16 18 20 22
TIME (HOURS)

FIGURE 13-A

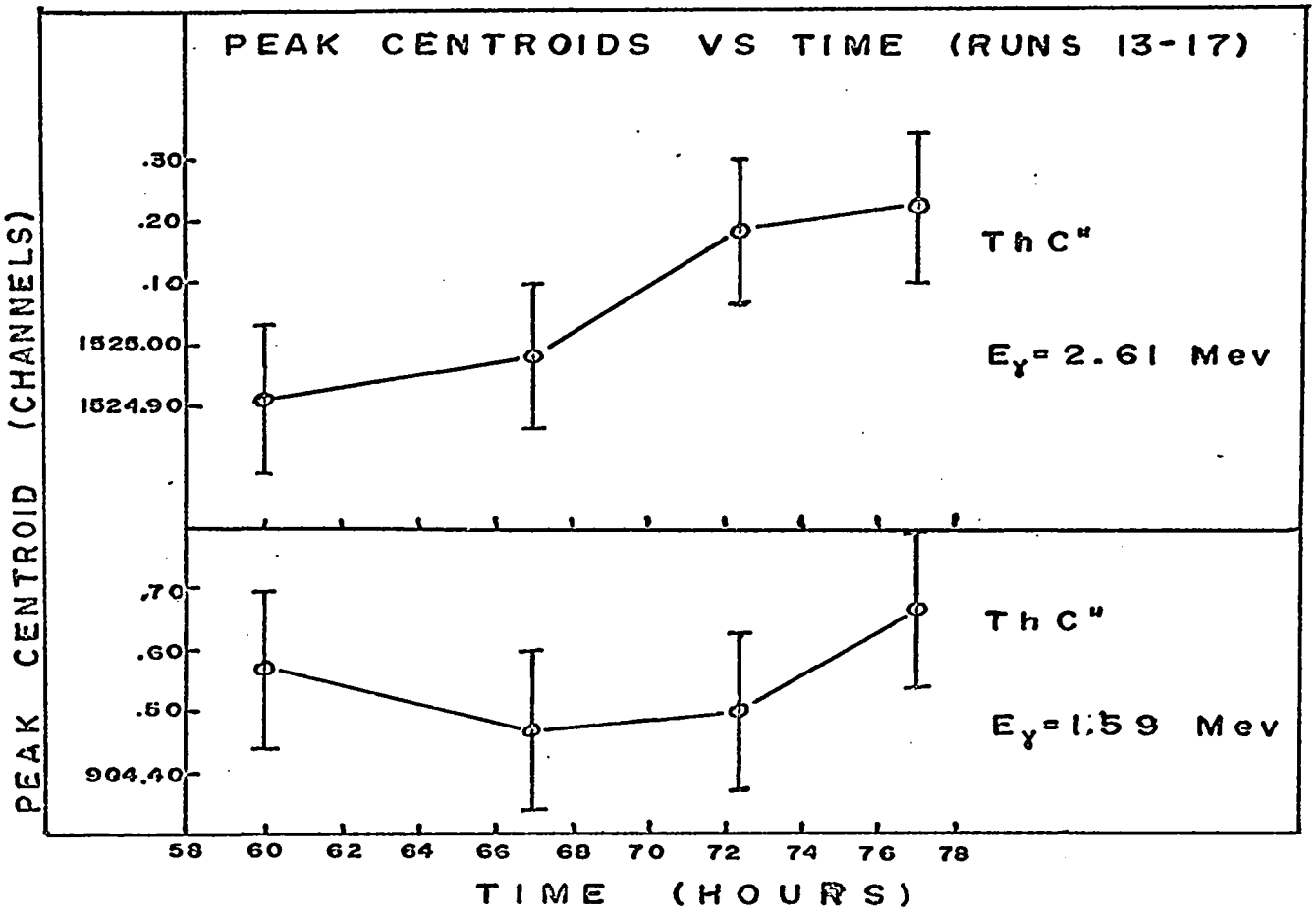
PEAK CENTROIDS VS TIME (RUNS 13-17)
PEAK CENTROID (CHANNELS)
.30
.20
.10
1525.00
1524.90
ThC"
E_γ= 2.61 Mev
.70
.60
.50
904.40
ThC"
E_γ= 1.59 Mev
58
60
62
64
66
68
70
72
74
76
78
TIME (HOURS)

FIGURE 13-B

CHAPTER 3

ANALYSIS OF RESULTS

3.1 The Doppler Shift Attenuation Method.

In the Doppler Shift Attenuation Method, the nucleus whose lifetimes are to be determined is made to recoil into a stopping medium, where its velocity varies with time in a manner which is characteristic of the combination of recoil ion and stopping material. The lifetime, τ, can be determined, if it is comparable to the slowing-down time for the ion in the medium, by measuring the change in energy between gamma-rays emitted at different angles with respect to a given direction.

It is desirable for the recoil ion to have as large an initial velocity V(0), so that large energy shifts can be measured. One can obtain this condition by using heavy ion bombardment or a reaction such as (α,n) just above the threshold energy ($\frac{V(0)}{c} \geq 1\%$). Also, if we have a large $\frac{V(0)}{c}$, the slowing down occurs in the electronic region, where the velocity function with time is relatively well known. Also, since we get large Doppler shifts, we can use NaI(Tl) detectors of high efficiency to obtain good statistics for the gamma-rays. However, the excited states that are populated are rather restricted, and there are kinematics difficulties involved with these reactions; in the case of (α,n) the outgoing neutron covers a spread of angles, thus introducing an uncertainty in the direction of the recoiling ion which emitted the gamma-ray.

More recently, lithium-drifted Germanium detectors have been used in proton capture reactions. Here, the direction of the recoil ion is the same as that of the incoming proton, and also a greater variety of levels can be populated. However, due to the small mass of the proton, the initial recoil velocity is much smaller $\left(\frac{v(o)}{o}\right) \approx .2\%$ in our case), thus the Doppler shifts are smaller. The Ge(Li) detectors, with relatively high resolution, can however detect the small energy changes involved, although their low efficiency diminishes the gamma-ray statistics. Also, the slowing down occurs in the atomic, or nuclear, region where the theory is not as well known as in the electronic case.

In the Doppler Shift Attenuation Method involving (p,γ) reactions, the proton is absorbed into a nucleus (A,Z) at the resonance energy, Ep, and the resulting nucleus, (A+1, Z+1) recoils with momentum equal to that of the incoming proton, and in the same direction. Starting with an initial velocity $V(o) = \frac{MpVp}{M}$,

M = mass of proton

Vp = velocity of incoming proton

the recoil ion then slows down in a "thick" material. The resonance level, in many cases, is very short lived ($<10^{-15}$sec) with respect to the slowing down time for the ion in the solid ($\approx 5 \times 10^{-13}$sec.) Thus the resonance level decays immediately to a bound level, whose lifetime we wish to determine, before the ion has started to slow down. Effectively, the bound level in question is populated directly. While the ion is slowing down in the solid (which, in our case is the target material itself) it

emits gamma-rays which may or may not be Doppler-shifted, depending on the lifetime of the level. By measuring the energy of the gamma-rays at two angles, θ_1 and θ_2 with respect to the beam direction, and, if the velocity of the ion as a function of time is known, one can determine the lifetime of the level, or at least set upper or lower limits (cf Figure 14).

If the lifetime of the level is very short lived with respect to the stopping time, or, if the nucleus recoils into vacuum, the gamma-ray emitted from that level will undergo a full, or unattenuated Doppler shift.

The energy of a gamma-ray, at a given angle θ is

$$E_\gamma(\theta) = E_\gamma(90^0) \left[1 + \frac{v_z}{c} \cos \theta\right] \quad \ldots\ldots\ldots\ldots\ldots\ldots (1)$$

In this case, the velocity $v_z = v(o)$ and does not change with time, therefore

$$E_\gamma(\theta) = E_\gamma(90^0) \left[1 + \frac{v(o)}{c} \cos \theta\right] \quad \ldots\ldots\ldots\ldots\ldots\ldots (2)$$

where $E_\gamma(\theta)$ = energy of a gamma-ray emitted at an angle θ with respect to the initial direction of motion of the nucleus (i.e. the proton beam)

v_z = component of the velocity of the recoil ion, in the direction of the proton beam, when the gamma-ray is emitted

$E_\gamma(90^0)$ = energy of gamma-ray emitted at 90^0

$v(o)$ = initial velocity of recoil ion

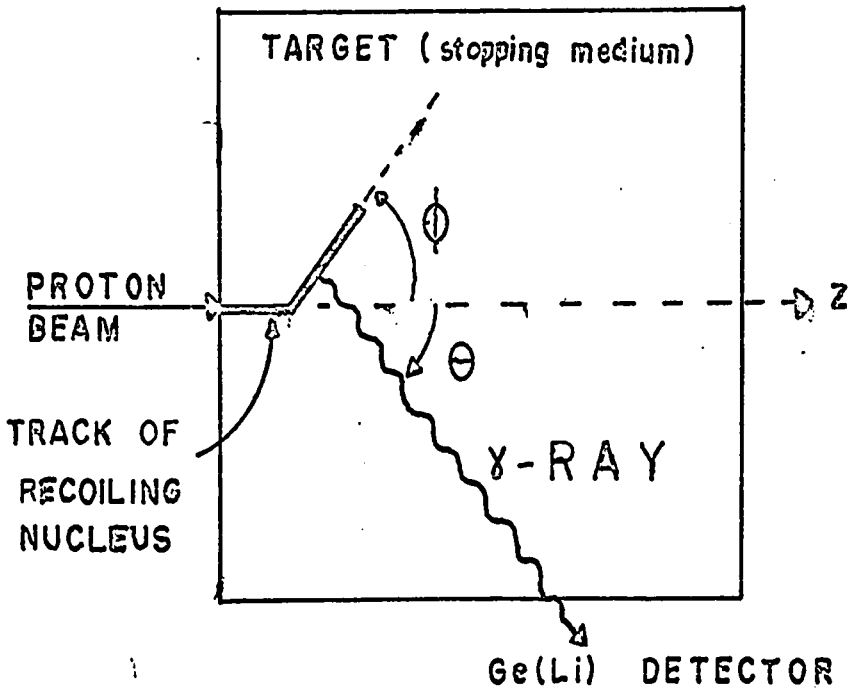

The recoiling nucleus first moves in the direction of the proton beam, then as it is slowed down, it suffers a change in direction, .During the slowing down of the nucleus, a gamma-ray is emitted at an angle Θ with respect to the beam axis.

FIGURE 14

Therefore, in this case, where $v_z = v(o)$ the gamma-rays detected at angles θ_1 and θ_2 will have a maximum energy shift (or full Doppler-shift) of

$$(\Delta E_\gamma)_{F.D.S.} = E_\gamma(90^o) \frac{v(o)}{c} [\cos \theta_1 - \cos \theta_2] \quad \ldots\ldots\ldots\ldots\ldots\ldots (3)$$

If now, the nucleus is made to recoil into a solid, the energy difference of gamma-rays emitted at θ_1 and θ_2 will lie between the limits of the equation 3 and zero, depending on the lifetime of the level as compared to the time it takes for the ion to stop in the medium

$$\Delta E_\gamma = E_\gamma(90^o)\frac{v(o)}{c}F(\tau) [\cos \theta_1 - \cos \theta_2] \quad \ldots\ldots\ldots\ldots\ldots\ldots (4)$$

where $o \leq F(\tau) \leq 1$ is the attenuation coefficient. If the lifetime is short with respect to the slowing down time of the ion in the solid, ($\tau \leq 10^{-15}$sec) then the gamma-rays are emitted when the recoil nucleus has full initial velocity and ΔE_γ is given by equation 3.

If the lifetime is long with respect to the stopping time, ($\tau \geq 10^{-11}$sec) then the gamma-rays are emitted when the recoil ion has come to a stop in the solid, i.e. $v_z = o$, $F = o$ and $\Delta E_\gamma = o$

But, if the lifetime lies inside these limits, the gamma-ray will be emitted when the nucleus has velocity $o < v_z < v(o)$ and the change in energy with angle will be given by equation 4, with $o < F < 1$. Thus, in this case, the lifetime of the level can be determined, if the attenuation coefficient F is known as a function of lifetime, τ.

The method is most sensitive when the lifetime is such that the attenuation coefficient is between .10 and .90 (corresponding to a lifetime $2X10^{-14}$sec $<\tau<10^{-12}$sec). If F is outside these limits, it is harder to assign a lifetime to a level, and limits are usually placed on the τ.

The experimental determination of the mean lifetime, τ, of an excited state consists of two stages. First, the attenuation coefficient, $F(\tau)$, is determined experimentally by observing the difference in the mean energy of a gamma-ray when it is detected at two angles, θ_1 and θ_2, and applying this difference in the form

$$F(\tau) = \frac{E_\gamma(\theta_1) - E_\gamma(\theta_2)}{E_\gamma(90^0)\frac{v(o)}{c}[\cos\theta_1 - \cos\theta_2]} \qquad \ldots\ldots\ldots\ldots\ldots\ldots(5)$$

Second, the lifetime is obtained from a calculated table of $F(\tau)$ as a function of τ, which is obtained from the velocity function of the recoil ion.

3.2 Theoretical Derivation of $F(\tau)$

The Doppler shift attenuation coefficient, $F(\tau)$, is first derived as a function of lifetime, τ, of the excited state and of the velocity of the recoil ion at the time it emits the gamma-ray. Then $F(\tau)$ is expressed as a function of the stopping power, $\frac{d\varepsilon}{d\rho}$, for the combination of recoil ion and stopping medium

A. Dependence of $F(\tau)$ on τ and on the Velocity of The Recoil Ion.

Suppose an excited nucleus, in state A, decays to state B, giving of γ_1, which in turn decays to a state C, giving off γ_2

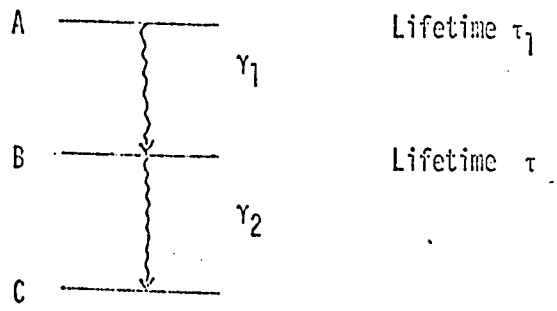

Also, suppose that initially, at time $t = 0$, the number of atoms in state A is $N_A = N_{Ao}$. The number of atoms at $t = 0$ in states B and C are $N_B = N_{Bo} = 0$ and $N_C = N_{Co} = 0$ respectively.

Then, at any later time, t, the number of atoms present in state A is

$$N_A = N_{Ao}\, e^{-t/\tau_1} \qquad \text{.....(6)}$$

Now, the rate of change in the number of atoms in state B is

$$\frac{dN_B}{dt} = \frac{N_A}{\tau_1} - \frac{N_B}{\tau} \qquad \text{.....(7)}$$

Therefore, the number of atoms N_B at time t is

$$N_B = \frac{\tau}{\tau_1 - \tau} N_{Ao} \left[\exp\left(-\frac{t}{\tau_1}\right) - \exp\left(-\frac{t}{\tau}\right) \right] \qquad \text{.....(8)}$$

and the number of atoms of type B decaying per unit time is

$$-\frac{N_B}{\tau} = \frac{N_{Ao}}{\tau_1-\tau}\left[\exp(-\frac{-t}{\tau_1}) - \exp(\frac{-t}{\tau})\right] \quad \text{.....(9)}$$

Also, the energy of a gamma-ray, γ_2, emitted at time t and angle θ is

$$E\gamma = E\gamma(90^0)\left[1 + \frac{\overline{V_z(t)}}{c}\cos\theta\right] \quad \text{.....(10)}$$

The average energy of a gamma-ray emitted at an angle θ is just the number of gamma-rays emitted at time t times the energy of that gamma-ray at time t and angle θ, integrated over all of time, and divided by the total number of gamma-rays emitted over all time, i.e.

$$\bar{E}\gamma(\theta) = \frac{\int_0^\infty \frac{N_{Ao}}{\tau_1-\tau}\left[\exp(-\frac{t}{\tau_1})-\exp(\frac{t}{\tau})\right]E\gamma(90^0)\left[1+\frac{\overline{V_z(t)}}{c}\cos\theta\right]dt}{\int_0^\infty \frac{N_{Ao}}{\tau_1-\tau}\left[\exp(-\frac{t}{\tau_1})-\exp(-\frac{t}{\tau})\right]dt} \quad \text{..(11)}$$

This reduces to

$$\bar{E}\gamma = E\gamma(90^0)\left\{1 + \frac{v(o)}{c}\cos\theta\left[\frac{\int_0^\infty \overline{v_z(t)}\left[\exp(-\frac{t}{\tau_1})-\exp(-\frac{t}{\tau})\right]dt}{(\tau_1-\tau)\,v(o)}\right]\right\} \quad (12)$$

where we have multiplied top and bottom of the expression on the right by v(o), the initial recoil velocity.

Since the average energy of a gamma-ray at an angle is

$$\bar{E}_\gamma(0) = E_\gamma(90^0)\left[1 + F(\tau)\frac{v(0)}{c}\cos\theta\right] \quad \ldots (13)$$

where $0 \leq F(\tau) \leq 1$

therefore, comparing equations (12) and (13), we see that

$$F(\tau) = \frac{1}{v(0)(\tau_1 - \tau)}\int_0^\infty \overline{V_z(t)}\left[\exp\left(\frac{-t}{\tau_1}\right) - \exp\left(\frac{-t}{\tau}\right)\right]dt \quad \ldots\ldots(14)$$

The extraction of nuclear lifetimes from measurements of attenuated Doppler shifts (i.e. where $0<F<1$) is dependent upon a knowledge of the average velocity of the nuclei as a function of time during which they are slowing down in the stopping medium.

In order to obtain the function $\overline{v(t)}$, a knowledge of the stopping function, $\frac{dE}{dx}$ for the appropriate ion in the target material is required. Since there are no experimental data available for the ions, stopping material and velocities used in the present work, theoretical estimates for $\frac{dE}{dx}$ are required. For this range of velocities, there are two distinct mechanisms which are important for the slowing down of the nuclei; one is electronic in origin and arises from energy lost in exciting or ejecting atomic electrons, and the other is atomic, and arises from the transfer of energy to translational motion of an atom as a whole. The atomic, or nuclear, contribution is particularly important at low velocities and as a consequence of the low momentum imparted to the recoiling nuclei, the greater part of energy is lost through this mechanism

In the range of velocities concerned, (i.e. $\frac{V(t)}{c} < \frac{1}{137}$) the data compiled by Northcliffe[12] show that the electronic stopping power is closely proportional to the velocity of the recoil ion. The constant of proportionality has been calculated by Lindhard, Scharff, and Schiott[13] and the values $\frac{dE}{dx}$ predicted agree with experimental values within about 20%. They have also derived a universal formula for the nuclear scattering cross-section from which the energy loss due to atomic collisions was calculated. With these two expressions it is possible to include both electronic and atomic contributions to the slowing down of the recoil ions in the target.

In equation 14 for $F(\tau)$, the term $\overline{v_Z(t)}$ is the component of the recoil ion velocity in the Z direction (i.e. proton beam direction). Since the atomic collisions cause the beam of recoiling nuclei to diverge, this produces a further attenuating effect. Thus $\overline{v_Z(t)}$ becomes $\overline{v(t) \cos \phi\,(t)}$ or approximately $\overline{v(t)}$ X $\overline{\cos \phi\,(t)}$ where $\overline{\cos \phi\,(t)}$ is the average of the cosine of the angles through which the recoiling nuclei have been scattered. Expressions have been derived by Blaugrund[14] for $\overline{v(t)}$ and $\overline{\cos \phi\,(t)}$, the latter requiring the use of the atomic scattering cross-section of Lindhard et al.

B. Slowing Down Mechanisms

A heavy charged particle travelling through matter loses energy mainly by Coulomb interaction with the entire target atoms, or with bound or free electrons. The two main processes are:

1. Coulomb interaction between the screened charge of the projectile nucleus and the screened target nuclei. This process is referred to as nuclear or atomic stopping but is nothing but Rutherford scattering between two charged nuclei modified by a proper nuclear screening. There is both loss of kinetic energy and large angle scattering, i.e., the collisions cause a change in direction of the recoil nuclei, and one must then calculate the projection of the recoil ion velocity along the proton beam axis, i.e. $\overline{v(t) \cos \phi(t)}$. This is called atomic stopping $(\frac{dE}{dx})_a$

2. Coulomb interaction between the screened projectile nucleus and the individual bound or free electrons in the target material. This is called electronic stopping, $(\frac{dE}{dx})_e$.

The total stopping power is the sum of these two contributions, i.e.

$$(\frac{dE}{dx}) = (\frac{dE}{dx})_a + (\frac{dE}{dx})_e \quad \ldots\ldots\ldots \quad (15)$$

The theory used in these experiments is that due to Blaugrund[14] who modified Lindhard, Scharff and Schiott's theory[13] to account for large angle scattering.

Dimensionless variables are used throughout the calculations.

ε = dimensionless energy

ρ = dimensionless distance

Lindhard, Scharff and Schiott have found, on the basis of Thomas-Fermi arguments, that, for velocities below $\frac{c}{137} Z_1^{2/3}$, where Z_1 = atomic number of recoil ion, the electronic stopping power is given by

$$\left(\frac{d\varepsilon}{d\rho}\right)_e = k\,\varepsilon^{1/2} \qquad \text{.....(16)}$$

where $$k = \frac{.0793\, Z_1^{1/2} Z_2^{1/2} (A_1 A_2)^{3/2}}{(Z_1^{2/3} + Z_2^{2/3})^{3/4} A_1^{3/2} A_2^{1/2}}\, \xi$$

where $\xi = Z_1^{1/6}$

and A = mass no.

and subscript 1 refers to recoil ion and subscript 2 refers to atom in stopping medium. It is seen that the expression for k is symmetric in Z_1 (projectile) and Z_2 (stopping material). However, from the work of Ormrod et al [15] it appears that the electronic stopping cross-section is not accurately described by the Lindhard formula, but that it shows oscillations around the Lindhard curve. The difference depends on Z_1 and is independent of Z_2. In the case of P^{31} ions stopping in Si^{30}, these effects lead to a correction of less than .5% (cf Engelbertink et al)[16]. Since the correction is independent of Z_2 and since Z_1 is the same in our case, P^{30}, therefore for P^{30} ions stopping in Si^{29}, the correction is probably also less than .5%. In any event, since in our case $\frac{v(o)}{c}$ = . 2%, the electronic slowing down contribution is much smaller than the atomic contribution.

For the atomic stopping power contribution, the equation due to Engelbertink et al[16] has been used to describe the curve given by Lindhard (Figure 1 in reference 13).

This equation is

$$\left(\frac{d\varepsilon}{d\rho}\right)_a = -.2 \log_{10}\left[\frac{\varepsilon^{1.215}}{70} + \frac{.002}{\varepsilon^{.815}}\right] \quad \ldots\ldots(18)$$

In Figure 15, equation (18) is plotted as a function of energy (solid curve). As can be seen, this curve quite accurately fits the calculations of Lindhard et al (dots) which are summarized in Schiott's article[11].

In dimensionless parameters, the total stopping power is again the sum of the electronic and nuclear contributions, i.e.

$$\left(\frac{d\varepsilon}{d\rho}\right) = \left(\frac{d\varepsilon}{d\rho}\right)_a + \left(\frac{d\varepsilon}{d\rho}\right)_e \quad \ldots\ldots\ldots\ldots(19)$$

Figure 16 shows the relative contributions of the atomic stopping power and the electronic stopping power (calculated for our case, in which $k = .224$) to the total stopping power.

Since there is some uncertainty as to the chemical composition of the target (i.e. proportion of Oxygen to Silicon atoms), calculations of $F(\tau)$ were therefore made for the extreme cases of Phosphorus ions in pure Silicon, and in Silicon dioxide. These functions are equal to within 2%, as is seen in Table 3.

A more detailed explanation of the stopping power, and its effect on the $F(\tau)$ vs τ curve is given in appendix A.

Also, the $F(\tau)$ vs τ curve for the Ep = 1505 Kev resonance in $Si^{29}(p,\gamma)P^{30}$, calculated for 50 Kev P^{30} ions slowing down in $Si^{29}O_2$ is shown in Figure 17.

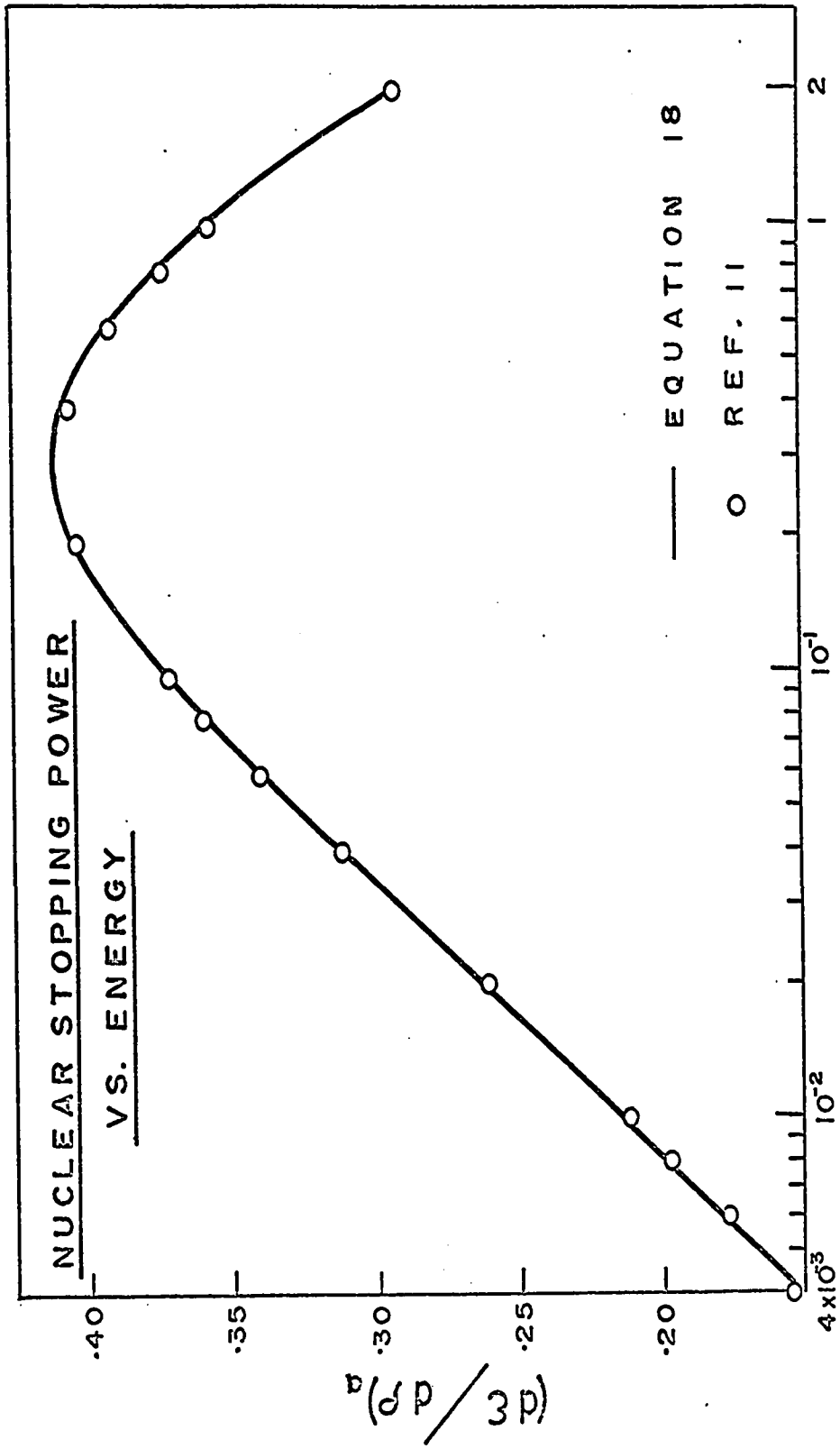
NUCLEAR STOPPING POWER
VS. ENERGY
EQUATION 18
O REF. 11
$(d\varepsilon/d\rho)_a$
ε
.40
.35
.30
.25
.20
4×10^{-3}
10^{-2}
10^{-1}
1
2

FIGURE 15

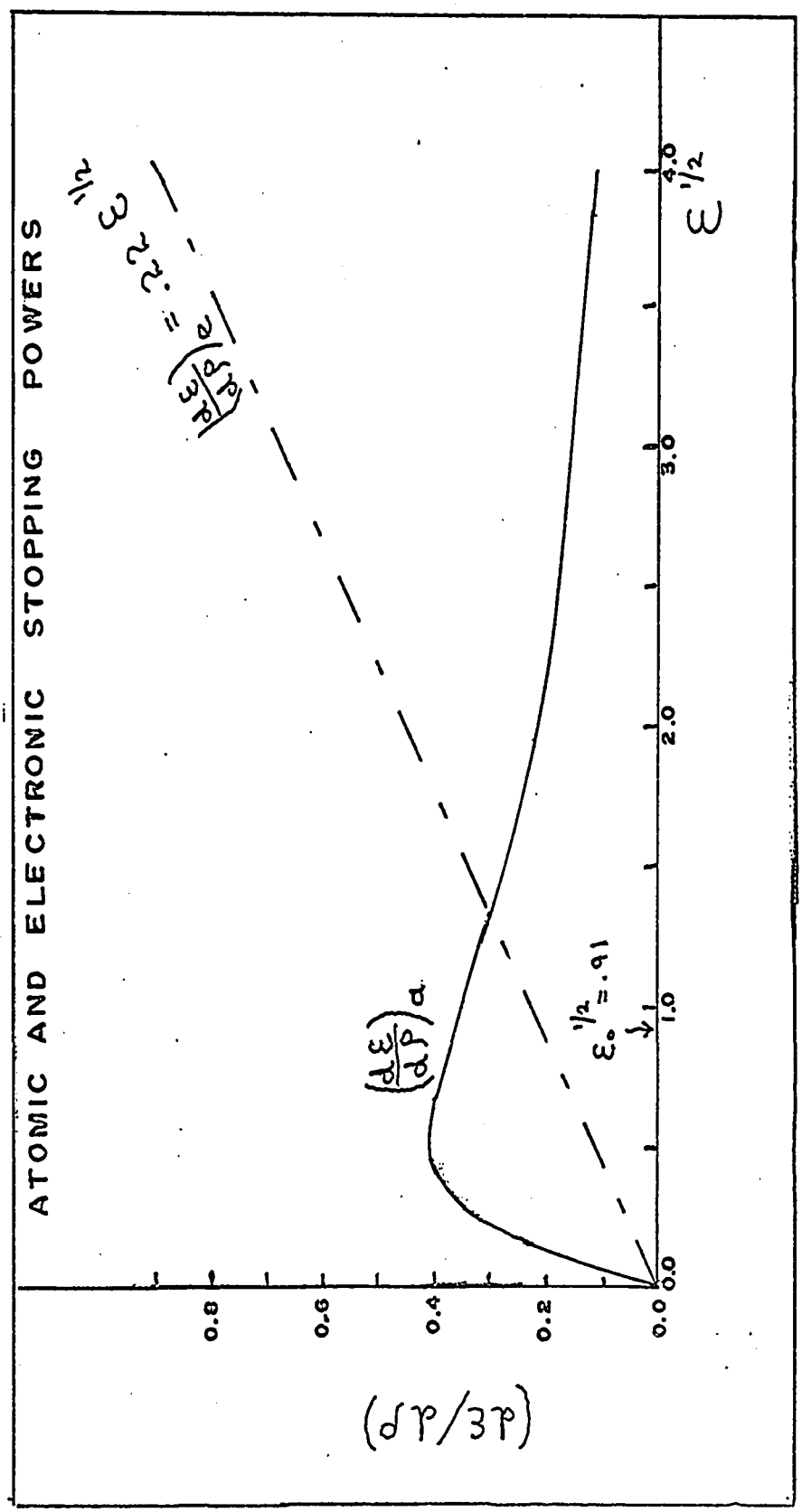
ATOMIC AND ELECTRONIC STOPPING POWERS
$\varepsilon^{1/2}$
$\varepsilon_0^{1/2} = .91$
$\left(\frac{d\varepsilon}{d\rho}\right)_e = 2.2\,\varepsilon^{1/2}$
$\left(\frac{d\varepsilon}{d\rho}\right)_n$
$(d\varepsilon/d\rho)$
0.0
0.2
0.4
0.6
0.8
1.0
2.0
3.0
4.0

FIGURE 16

TABLE III

Slowing Down of 56 Kev P^{30} Ions in Si^{29} and in $Si^{29}O_2$: Effect on $F(\tau)$.

τ ($\times 10^{-15}$ sec.)	$F(\tau)$ for E_p 1686 Kev	
	P^{30} in Si^{29}	P^{30} in $Si^{29}O_2$
1	.994	.994
2	.988	.989
4	.976	.978
6	.965	.966
8	.953	.955
10	.942	.944
20	.886	.890
40	.783	.788
60	.696	.699
80	.622	.624
100	.561	.562
200	.371	.370
400	.219	.217
600	.155	.153
800	.120	.118
1000	.098	.096
2000	.051	.050
4000	.026	.026
6000	.017	.017
8000	.013	.013
10000	.011	.011

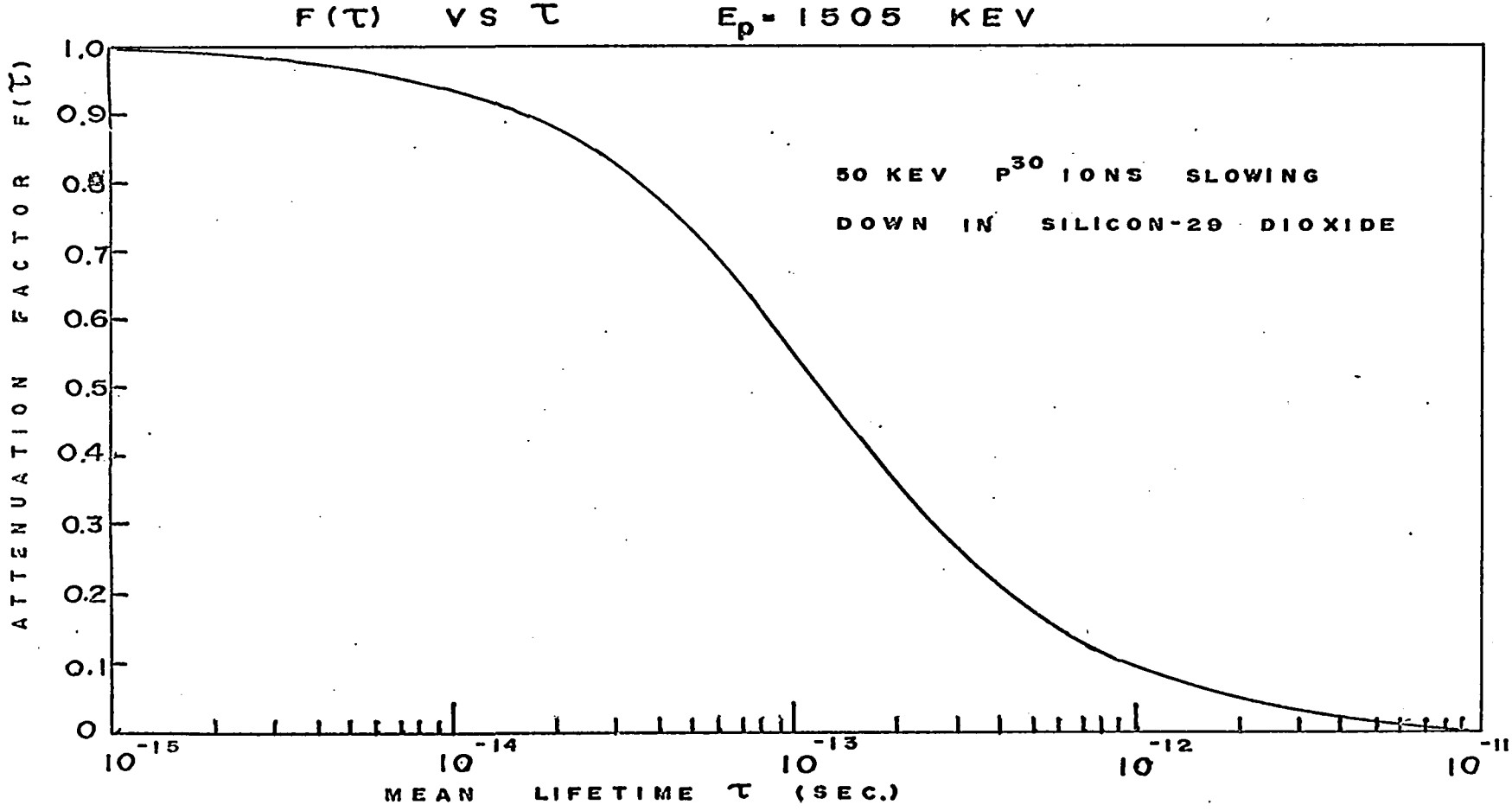
F(τ) VS τ
E_p = 1505 KEV
50 KEV P^{30} IONS SLOWING
DOWN IN SILICON-29 DIOXIDE
ATTENUATION FACTOR F(τ)
1.0
0.9
0.8
0.7
0.6
0.5
0.4
0.3
0.2
0.1
0
10^{-15}
10^{-14}
10^{-13}
10^{-12}
10^{-11}
MEAN LIFETIME τ (SEC.)

FIGURE 17

3.3 Statistical Errors in The Peak Centroids

The attenuation coefficient,

$$F(\tau) = \frac{E_\gamma(\theta_1) - E_\gamma(\theta_2)}{E_\gamma(90^0)\,\frac{v(o)}{c}\,[\cos\theta_1 - \cos\theta_2]}$$

contains uncertainties due to the determination of the centroids.

Since $E_\gamma = Ax + B$ (to first order) ..... (20)

where A = dispersion in Kev/channel

and x = channel number

and B = channel zero energy.

therefore

$$F(\tau) = \frac{A(\bar{x}_1 - \bar{x}_2)}{(\Delta E_\gamma)_{F.D.S.}} \quad \ldots\ldots\ldots\ldots\ldots \quad (21)$$

where $\bar{x}_1$ = centroid (in channels) of gamma-ray emitted at θ_1

$\bar{x}_2$ = centroid (in channels) of gamma-ray emitted at θ_2

and $(\Delta E_\gamma)_{F.D.S.}$ = full Doppler shift energy

$$= E_\gamma(90^0)\,\frac{v(o)}{c}\,[\cos\theta_1 - \cos\theta_2] \quad \ldots\ldots\ldots \quad (22)$$

The standard deviation in a function $R = F(x_1, x_2 \ldots x_n)$ is

$$\sigma = \sqrt{\sum_{i=1}^{n} \left(\frac{\partial R}{\partial x_i}\right)^2 (\Delta x_i)^2} \quad \ldots\ldots\ldots\ldots\ldots \quad (23)$$

Thus, for $F(\tau)$ this is

$$\Delta F(\tau) = \frac{A\sqrt{\Delta x_1^2 + \Delta x_2^2}}{(\Delta E_\gamma)_{F.D.S.}} \quad \text{..... (24)}$$

Now, the errors Δx_1 and Δx_2 in the centroids x_1 and x_2 can be evaluated by applying equation (23) to them also. Since

$$\bar{x} = \frac{\sum_{i=1}^{n} x_i N_i}{\sum_{1}^{n} N_i} = \frac{\sum_{1}^{n} x_i (N_{Ti} - N_{Bi})}{\sum_{1}^{n} (N_{Ti} - N_{Bi})} \quad \text{.....(25)}$$

where x_i = i^{th} channel number in peak

and N_i = number of counts in the peak

and N_{Ti} = total number of counts in i^{th} channel.

N_{Bi} = number of counts in i^{th} channel due to background only.

therefore $\bar{x}$ is a function of $2n$ variables, the N_{Ti} and the N_{Bi}, where n is the number of channels over which the centroid is evaluated. Therefore,

$$(\Delta\bar{x})^2 = \sum_{j=1}^{n}\left[\left\{\frac{\partial}{\partial N_{Tj}}\left[\sum_{i=1}^{n} x_i (N_{Ti} - N_{Bi})\right]\left[\sum_{1}^{n} (N_{Ti} - N_{Bi})\right]^{-1}{}^{2}\right\}\{(\Delta N_{Tj})\}^2\right]$$

$$+ \sum_{j=1}^{n}\left[\left\{\frac{\partial}{\partial N_{Bj}}\left[\Sigma x_i (N_{Ti} - N_{Bi})\right]\left[\Sigma (N_{Ti} - N_{Bi})\right]^{-1}{}^{2}\right\}\{(\Delta N_{Bj})\}^2\right]$$

.....(26)

which reduces to

$$\Delta\bar{x} = \frac{1}{N}\sqrt{\sum_{k=1}^{n}(\bar{x} - x_k)^2(N_{Tk} + N_{Bk})} \qquad \text{.....(27)}$$

where N = total number of counts in the peak (with background subtracted)

In some cases, more than one value for $F(\tau)$ was obtained for a given level. Then, the weighted mean

$$\bar{F} = \frac{\Sigma \frac{Fi}{\sigma_i^2}}{\Sigma \frac{1}{\sigma_i^2}} \qquad \text{.....(28)}$$

was used, where σ_i is the standard deviation in the i^{th} value of F. The error in this mean is

$$\Delta\bar{F} = \frac{1}{\sqrt{\Sigma \frac{1}{\sigma i^2}}} \qquad \text{.....(29)}$$

3.4 Analysis of the Gamma-Ray Spectra

The resonances investigated were done at least twice at both θ_1 and θ_2, except for the Ep = 1773 - 1775 Kev resonances, which were done only once at each angle. The different runs are numbered 1 to 17.

A. The Ep = 1505 Kev Resonance

The first $Si^{29}(p,\gamma)P^{30}$ resonance studied in detail for measurements was that for Ep = 1505 Kev, corresponding to an excitation energy of Ex = 7.052 Mev in P^{30}. This resonance was done in two groups of runs,

#1 (90^0) and #2 (0^0), and #13 (0^0) and #15 (90^0). The recoil ion had an initial velocity of $\frac{v(o)}{c} = 1.90 \times 10^{-3}$, and since the runs were done at 0^0 and 90^0, then

$$\left(\frac{\Delta E_\gamma}{E_\gamma}\right)_{F.D.S.} = 1.90 \times 10^{-3}$$

The gamma-rays of interest are those whose energies are 3.171, 2.821, and 2.257 Mev, corresponding to transitions between the levels 4.624 →1.453, R→4.231, and 4.231→1.974 Mev respectively. The 2.821 Mev gamma-ray, observed at 0^0, should show the full Doppler shift i.e. $F(\tau) = 1$ since the mean lifetime of the resonance is $<10^{-15}$sec (cf. Endt & Van der Leun;[5] Harris[8]). The observation of the full shift of this primary gamma-ray serves the dual purpose of establishing the stability of the apparatus against electronic drift, and of providing a reference with which the shift of the secondary gamma-ray can be compared.

Spectra were thus obtained at 0^0 and at 90^0, and the Doppler shifts of the two secondary gamma-rays were determined. The gamma-ray spectrum of this resonance, at $\theta = 90^0$, is shown in figure 18.

In runs #1 and #2, the 2.821 Mev gamma-ray, and its second escape peak show full shifts of $F = .96 \pm .04$, and $F = 1.01 \pm .08$ respectively, corresponding to an average $\bar{F} = .97 \pm .03$. The 2.257 Mev γ -ray, and its second escape peak, show shifts of $0.12 \pm .22$ Kev and $0.39 \pm .79$ Kev respectively, corresponding to $F = .03 \pm .05$, and $.09 \pm .18$ respectively.

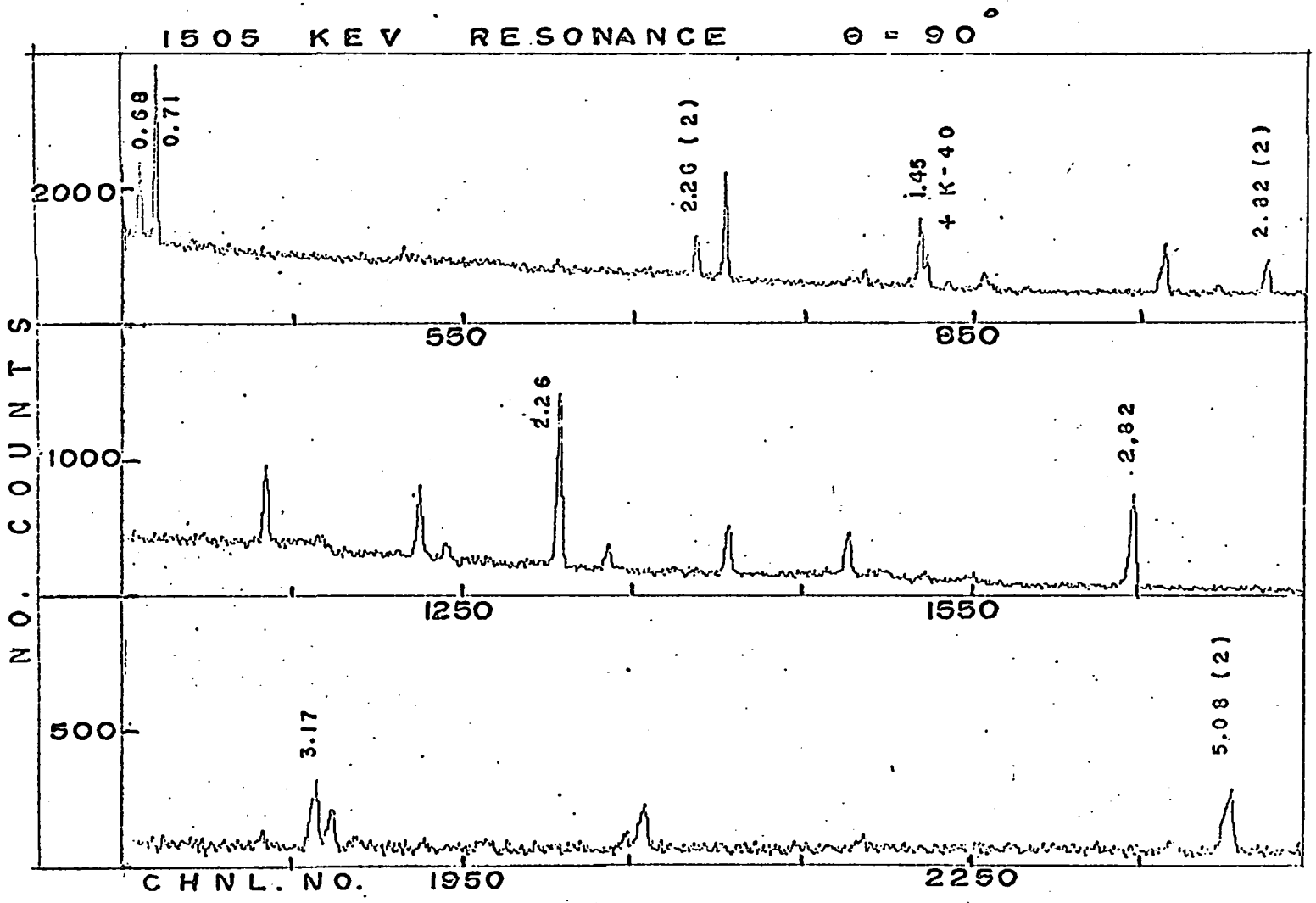
1505 KEV RESONANCE θ = 90°
0.68
0.71
2.26 (2)
1.45
+ K-40
2.82 (2)
2000
550
650
NO. COUNTS
2.26
2.82
1000
1250
1550
3.17
5.08 (2)
500
CHNL. NO.
1950
2250

FIGURE 18

In runs # 13 and # 15, the 2.821 Mev gamma-ray, and its second escape peak showed full shifts of .97 ± .03 and 1.00 ± .05 respectively. The 2.257 Mev gamma-ray and its second escape peak displayed shifts of .20 ± .15 Kev (F = .05 ± .04) and .31 ± .41 Kev (F = .07 ± .09) respectively. In these runs, the 3.171 Mev x-ray, de-exciting the 4.62 Mev level was strong enough to permit observation of an attenuated shift of 2.03 ± .34 Kev, corresponding to F = .34 ± .09.

The mean lifetime of the 4.231 Mev level was thus found to be $\tau = 2000 \begin{smallmatrix} + 3000 \\ - 800 \end{smallmatrix}$ fs, while that for the 4.624 Mev level was found to be $\tau = 215 \begin{smallmatrix} + 105 \\ - 65 \end{smallmatrix}$ fs.

The errors quoted on all lifetimes were obtained only from the experimental uncertainties in the centroids of the respective peaks in the spectra. No estimate of the errors contributed by the uncertainties in the stopping and scattering calculations have been included since these calculations have not been tested experimentally. No gain drifts, within the experimental accuracy, were detected during these runs, as is displayed in Figure 19. In this Figure, the 90^0 - 0^0 experimental centroid shift is plotted against the cosine of the angle of detection of the gamma-ray. The straight line represents the full Doppler shift, calculated from equation (3). In the bottom half of the Figure, the experimental centroid shift for the 2.821 Mev gamma-ray (R→4.231 Mev) and its second escape peak are shown. In the upper half of the Figure, the shifts for the 2.257 Mev gamma-ray (4.231 → 1.974 Mev) and for the 3.171 Mev gamma-ray (4.624 → 1.453 Mev) are shown. The results obtained from this resonance are summarized in Table 4.

DOPPLER SHIFTS IN 1505 KEV RESONANCE

(RUNS 13(0°) AND 15(90°))

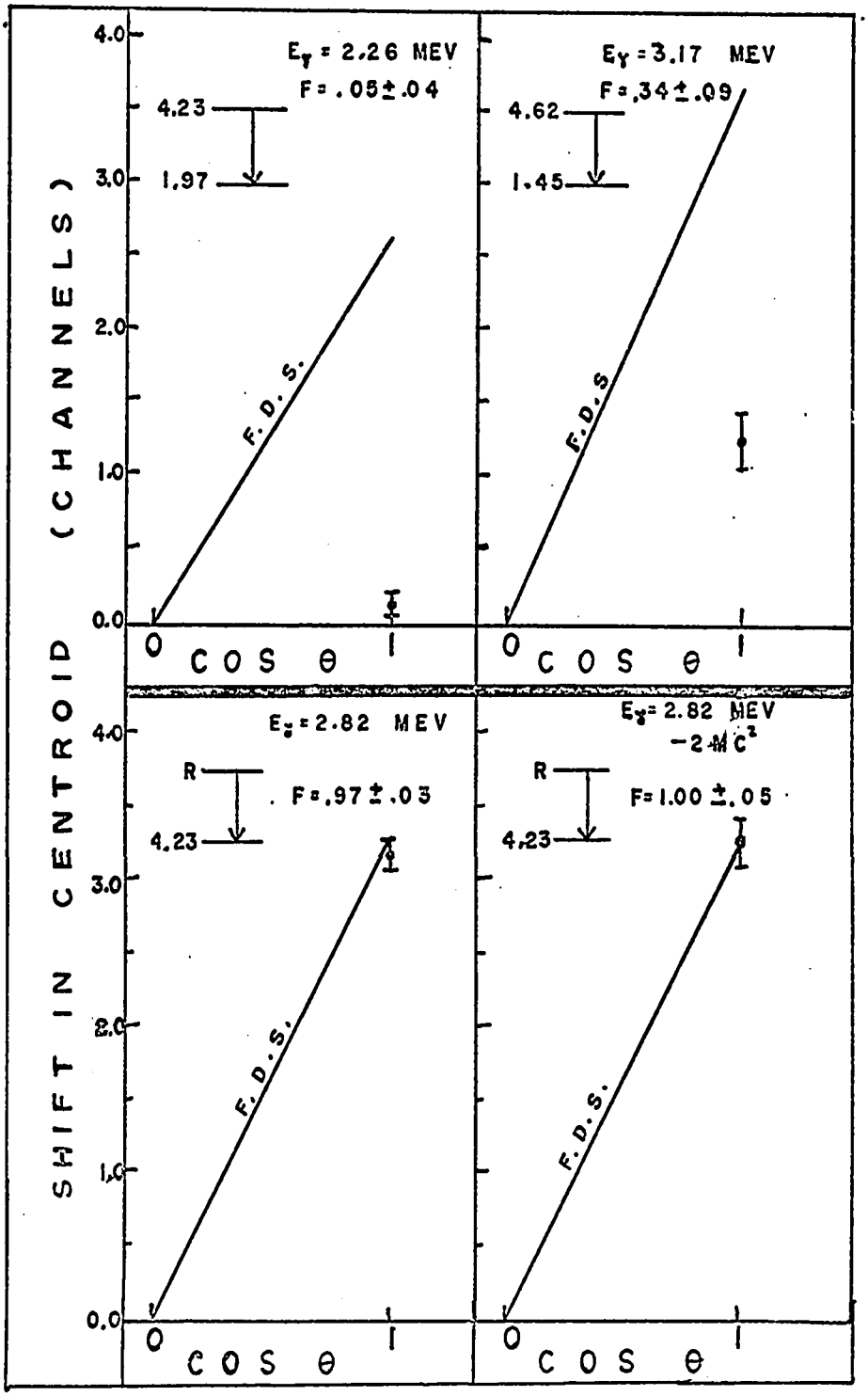

FIGURE 19

TABLE IV

Results of the E_p=1505 Kev Resonance.

Transition	E_γ (Mev)	ΔE_γ (Kev)	$(\Delta E_\gamma)_{f.d.s.}$ (Kev)	$F(\tau)$ (%)	$\overline{F(\tau)}$ (%)	τ (fsec)
R→4.231	2.821	5.15±.26	5.36	96±4		
		5.20±.2	5.36	97±3		
					98±3	full shift
	2.821 (2)	5.43±.6	5.36	101±8		
		5.36±.4	5.36	100±5		
4.231→1.974	2.257	.12±.22	4.29	3±5		
		.20±.15	4.29	5±4		
					5±3	2000^{+3000}_{-800}
	2.257 (2)	.39±.79	4.29	9±18		
		.31±.41	4.29	7±8		
4.624→1.453	3.171	2.03±.34	6.02	34±9		215^{+105}_{-65}

B. The Ep = 1643 Kev Resonance

The initial recoil velocity was $\frac{v(o)}{c} = 1.97 \times 10^{-3}$ (recoil energy of 54.8 Kev), and since the shifts were taken at 0^0 and 120^0, $(\frac{\Delta E_\gamma}{E_\gamma})_{F.D.S.} = 2.96 \times 10^{-3}$. This resonance was done in four consecutive runs at 0^0 (#9, #11) and at 120^0 (#10 and #12). The $\theta = 0^0$ spectrum for this resonance, corresponding to an excitation energy Ex = 7.190 Mev in P^{30}, is given in Figure 20.

The gamma-rays of interest are those of energy 2.338 and 0.709 Mev, corresponding to transitions between the levels 3.020 → 0.678 and 0.709 → 0 Mev respectively. These levels were populated directly from the resonance level which, according to Harris, and Endt and Van der Leun, has a width of $\Gamma = 17.2 \pm 2.0$ Kev, corresponding to a lifetime $\tau \leq 3 \times 10^{-20}$ sec, therefore no correction needed to be made to the attenuation coefficients.

Radioactive sources such as Co^{60} and ThC", and the gamma-rays arising from the resonance, at a given angle, provided a check as to the stability of the electronics. No drifts were observed within the experimental accuracy.

In runs #9 (0^0) and #10 (120^0), the 2.338 Mev gamma-ray displayed a full shift of 6.99 ± .64 Kev, corresponding to F = 1.01 ± .09, while the 0.709 Mev gamma-ray showed a shift of 0.00 ± .16 Kev, i.e. F = 0.00 ± .07.

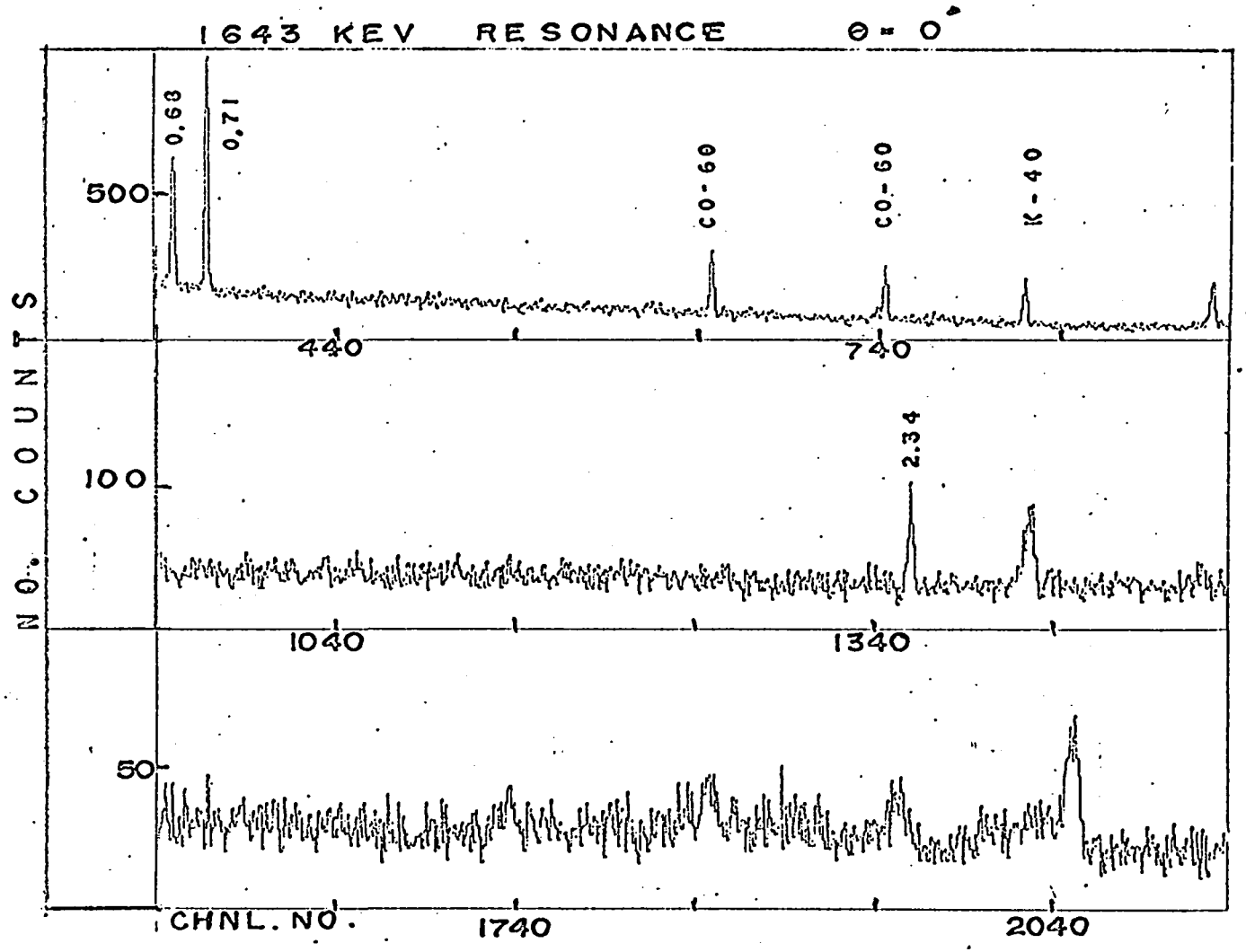
1643 KEV RESONANCE θ = 0°
0.68
0.71
CO-60
CO-60
K-40
500
440
740
NO. COUNTS
2.34
100
1040
1340
50
CHNL. NO.
1740
2040

FIGURE 2.0

TABLE V

RESULTS OF THE E_p=1643 Kev RESONANCE.

Transition	E_γ (Mev)	ΔE_γ (Kev)	$(\Delta E_\gamma)_{fds}$ (Kev)	$F(\tau)$ (%)	$\overline{F(\tau)}$ (%)	τ (fsec)
3.02→.678	2.338	6.99±.64	6.94	101±9	103±11	≤14
		7.75±1.2	6.94	111±18		
0.709→0	0.709	0.00±.16	2.10	0±7	4±5	≥1100
		0.18±.14	2.10	9±7		

In runs #11 (0^0) and #12 (120^0), the 2.338 Mev line shifted by 7.75 ± 1.2 Kev (F = 1.11 ± .18) while a 0.18 ± 14 Kev shift (F = .09 ± .07) was observed for the .709 Mev line.

Thus, for the 3.02 Mev level, a mean value $\overline{F}$ = 1.03 ± .11 was observed, leading to a lifetime $\tau \leq 14$ fs, while for the 0.709 Mev level, $\overline{F}$ = .04 ± .05, corresponding to $\tau \leq 1100$ fs. Table 5 provides a summary for the results obtained with this resonance.

C. The Ep = 1686 Kev Resonance.

This resonance was done in four consecutive runs at alternate angles $\theta_1 = 0^0$ and $\theta_2 = 120^0$, in an attempt to uncover any drifts in gain. The $\theta = 0^0$ spectrum, corresponding to an excitation energy Ex = 7.233 Mev in P^{30} is given in Figure 21. The initial recoil velocity of the P^{30} ions was $\frac{v(o)}{c} = 2.00 \times 10^{-3}$, and since the shift was taken between 0^0 and 120^0, $\left(\frac{\Delta E\gamma}{E\gamma}\right)_{F.D.S.} = 3 \times 10^{-3}$.

The gamma-rays of interest are those of 3.085 and 4.142 Mev, resulting from the transitions between the levels R → 4.142 and 4.142 → 0 Mev respectively.

In the first two runs, #4 (0^0) and #5 (120^0) no drifts were observed in the peak centroids. The 3.085 Mev line and 2nd escape peak which should display a full Doppler shift, did in effect shift by 9.62 ± .30 Kev and 9.15 ± .36 Kev respectively, corresponding to F = 1.04 ± .03 and F = .99 ± .04. The 4.14 Mev line and its second escape peak shifted by 9.94 ± .33 Kev (F = .80 ± .03) and 9.62 ± .33 Kev (F = .77 ± .03) respectively.

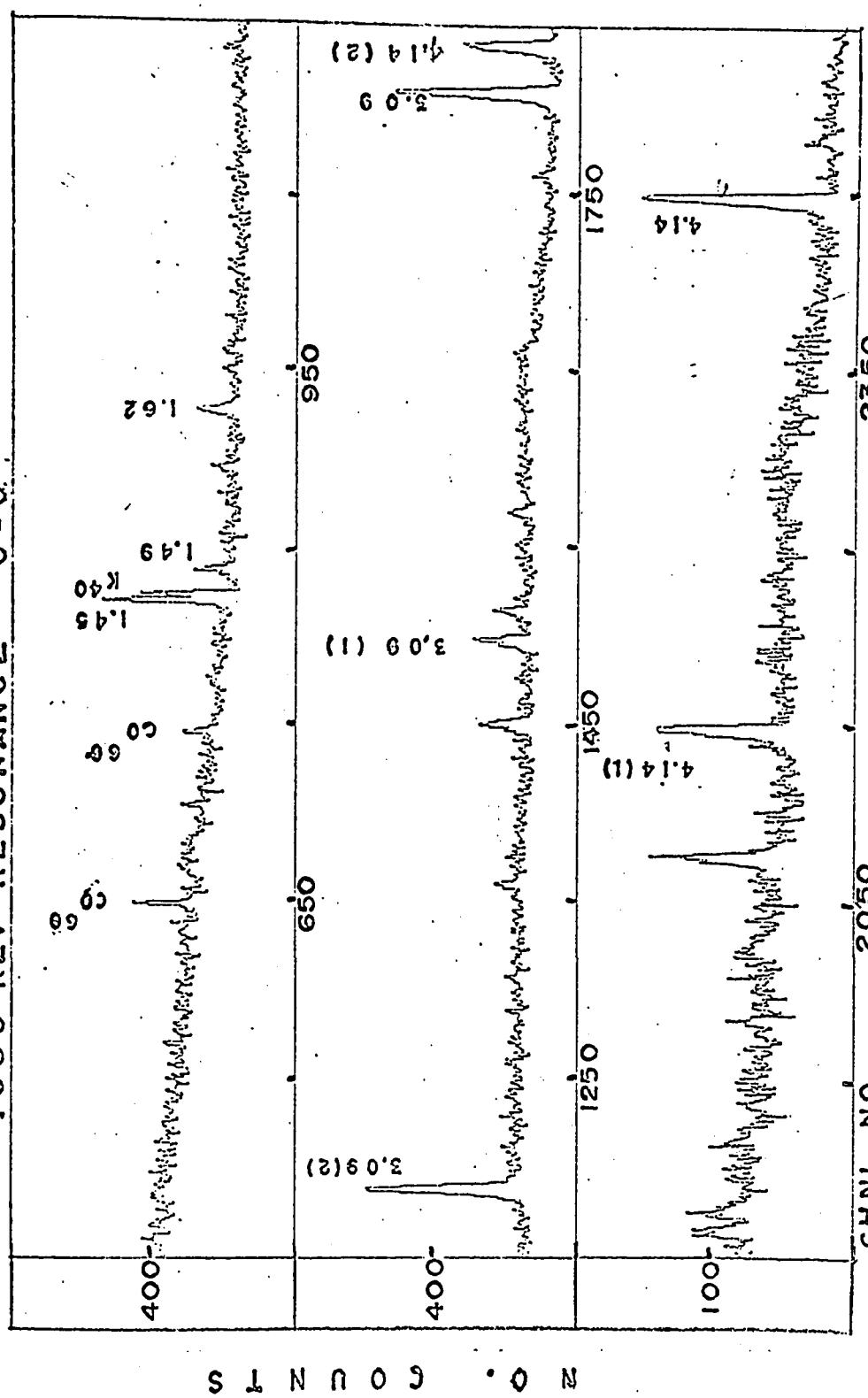
1'686 KEV RESONANCE θ = 0°
NO. COUNTS
CHNL. NO.
400
100
650
950
1250
1450
1750
2050
2350
1.62
1.49
1.43
1.40
3,09 (2)
3,09 (1)
4,14 (1)
4,14 (2)
4,14

FIGURE 21

In the second run, #7 (0^0) and #8 (120^0), a drift was observed in the peak centroids of the resonance gamma-rays. The 3.085 Mev gamma-ray, which should have shifted by 9.26 Kev, displayed a shift of 8.43 ± .25 Kev, leading to F = .91 ± .03, while its second escape peak shifted by 8.75 ± .40 Kev or F = .94 ± .04. Figure 22 shows the 0^0 - 120^0 experimental centroid shifts for the 3.085 Mev and second escape gamma-rays. The straight line is the calculated full Doppler shift (equation 3). On the left hand side of the figure, the results for runs #4 and #5 (no drifts) are given, while on the right hand side, the results for runs #7 and #8 are shown. As can be seen, drifts of .5 channels (.8 Kev) and .3 channels (.5 Kev) were observed in the centroids of the 3.085 Mev gamma-ray and its second escape peak, respectively. Since the second escape peak of the 4.14 Mev gamma-ray (4.14 → 0) is 3.12 Mev (only 40 Kev away from the 3.085 Mev line) a correction of .5 channels (.8 Kev) was therefore applied to its centroid in run #8, leading to a corrected shift of 10.25 ± .46 Kev (F = .82 ± .04).

As a result, the 4.142 Mev level was found to have a mean $\overline{F}$ = .80 ± .03, corresponding to a lifetime τ = 38 ± 7 fs.

Figure 23 shows the Doppler shift in the centroid of the 4.142 Mev second escape peak (E_γ = 3.120 Mev) (4.142→ 0 Mev transition), along with that of the 3.085 Mev gamma-ray (R → 4.142 Mev) for runs #4 and #5 (no gain drifts)

Table 6 summarizes the results obtained with this resonance.

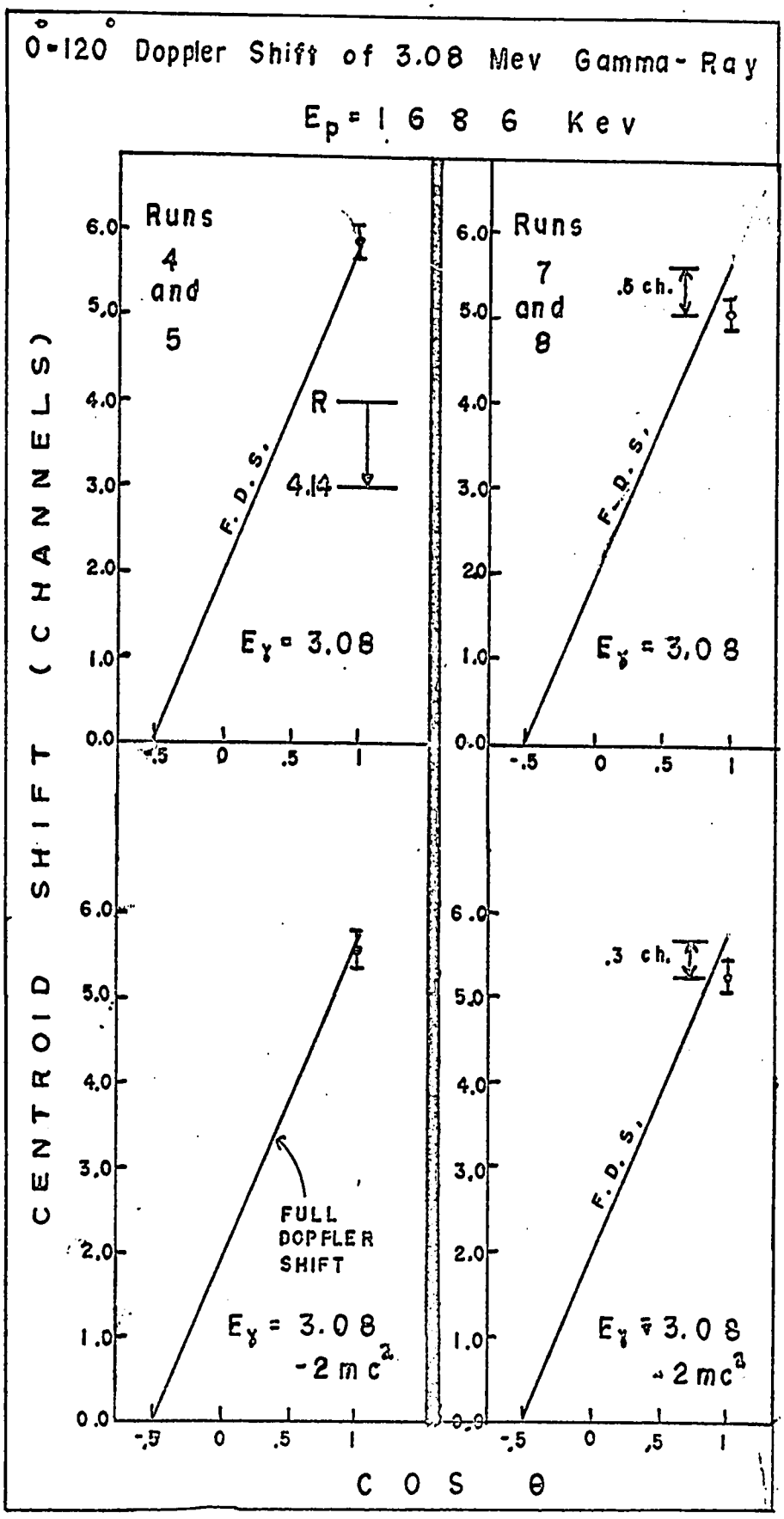
0°-120° Doppler Shift of 3.08 Mev Gamma-Ray
E_p = 1686 Kev
CENTROID SHIFT (CHANNELS)
Runs 4 and 5
Runs 7 and 8
R
4.14
F.D.S.
E_γ = 3.08
.5 ch.
.3 ch.
FULL DOPPLER SHIFT
E_γ = 3.08 - 2 mc²
E_γ = 3.08 + 2 mc²
COS θ

FIGURE 22

DOPPLER SHIFTS OF 3·085 Mev AND
4·142 Mev (SECOND ESCAPE) GAMMA-RAYS

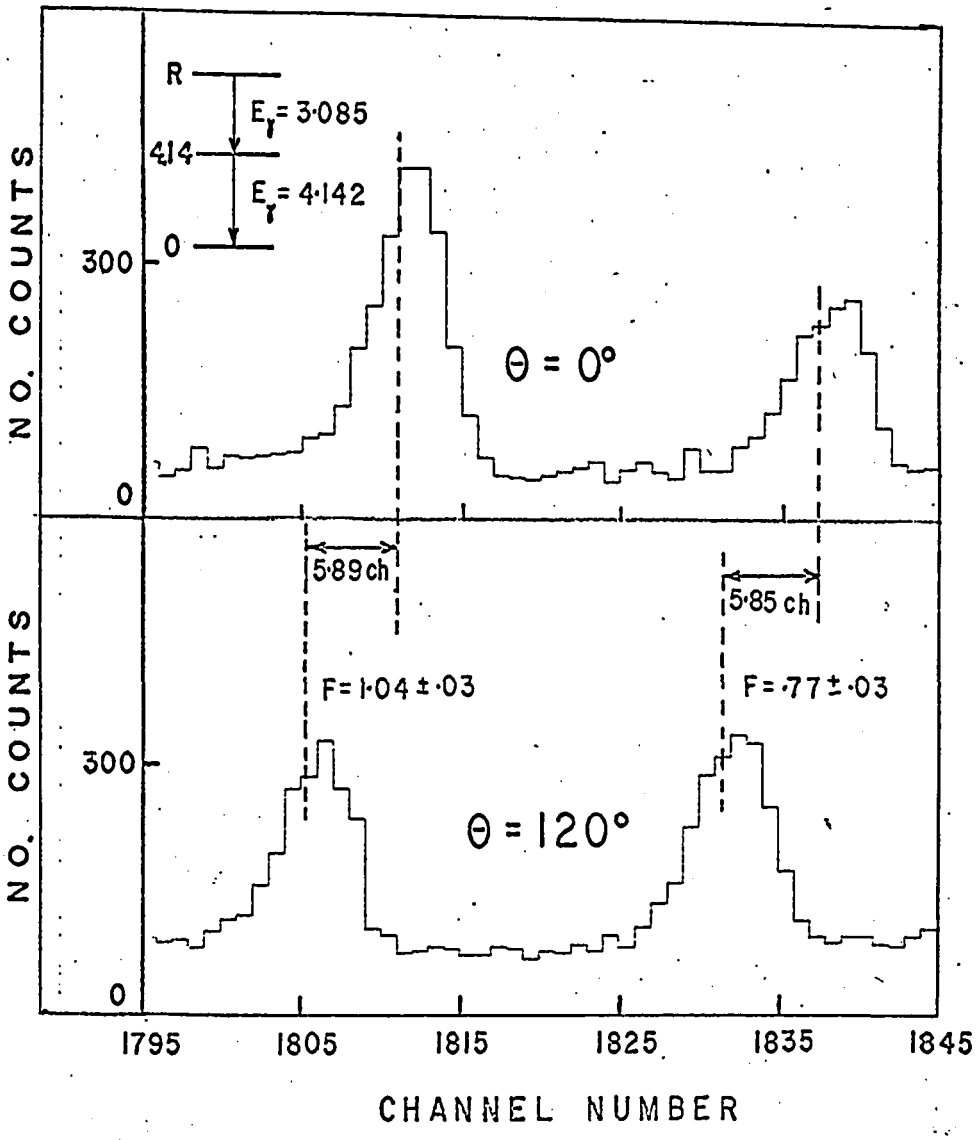

FIGURE 23

TABLE VI

Results of the E_p=1686 Kev Resonance.

A - Runs #4 and #5.

Transition	E_γ (Mev)	ΔE_γ (Kev)	$(\Delta E_\gamma)_{fds}$ (Kev)	$F(\tau)$ (%)	$\overline{F(\tau)}$ (%)	τ (fsec)
R→4.142	4.142	9.62±.30	9.26	104±3		full shift
	3.085 (2)	9.15±.36	9.26	99±4		
4.142→0	4.142	9.94±.33	12.43	80±3	80±3*	38±7
	4.142 (2)	9.62±.33	12.43	77±3		

B - Runs #7 and #8.

Transition	E_γ (Mev)	ΔE_γ (Kev)	ΔE_γ corr. (Kev)	$(\Delta E_\gamma)_{fds}$ (Kev)	$F(\tau)$ (%)	τ (fsec)
R→4.142	3.085	8.43±.25		9.26	91±3	
	3.085 (2)	8.75±.40		9.26	94±4	
4.142→0	4.142 (2)	9.43±.46	10.25±.46	12.43	82±4	38±7

*The value $\overline{F(\tau)}$= 80±3 is the average of the $F(\tau)$ values for both sets of runs, #4-#5 and #7-#8.

D. The Ep = 1773 Kev and 1775 Kev Doublet

These two resonances were done simultaneously at both 0^0 and 90^0 (cf. Figure 24 for the $\theta = 90^0$ spectrum) The initial recoil velocity of the P^{30} ions was $\frac{v(o)}{c} = 2.06 \times 10^{-3}$ (recoil energy E_R = 59.1 Kev) and $(\frac{\Delta E\gamma}{E\gamma})_{F.D.S.} = 2.06 \times 10^{-3}$.

i) Ep = 1773 Kev Resonance (Ex = 7.311 Mev)

The gamma-rays of interest are those at 2.810, 5.337, 6.602, 1.974, 3.048 and 3.473 Mev, corresponding to transitions between the levels 7.311→4.501, 7.311→1.974, 7.311→0.709, 1.974→0, 4.501→1.453, and 4.182→.709 Mev respectively.

The width of this resonance is given as $\Gamma \leq 1.5$ Kev by Harris et al[8], corresponding to a lifetime $\tau \geq 4 \times 10^{-19}$sec. The 2.810 and 6.602 Mev (second escape peak) resonance gamma-rays showed Doppler shifts corresponding to F = 1.03 ± .11 and F = 1.05 ± .05 respectively, leading to a mean value of $\bar{F}$ = 1.04 ± .05, and indicating that this resonance is very short-lived ($\tau_1 < 10^{-15}$sec).

However, the 5.337 Mev gamma-ray (second escape peak, which represents decay to the 1.974 Mev level, showed a Doppler shift of F = .96 ± .04. The 1.974 Mev level is also populated, according to Harris et al[8], by the Ep = 1775 Kev resonance, which, according to our results seems to have an attenuated Doppler shift. (cf following section on the 1775 Kev resonance) This could explain why F = .96 ± .04 for the 5.337 Mev γ-ray.

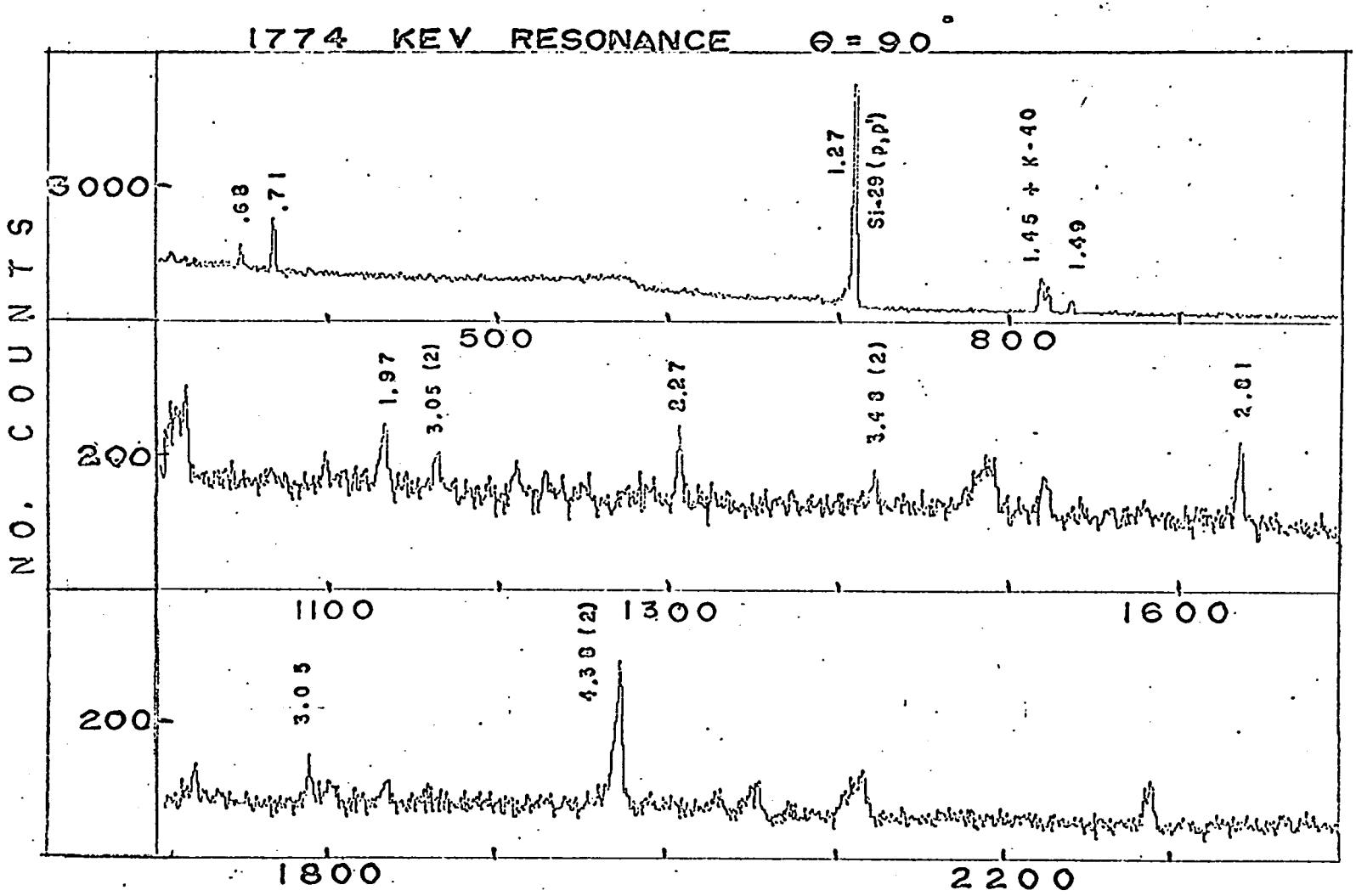
1774 KEV RESONANCE θ = 90°
NO. COUNTS
3000
200
200
.68
.71
1.27
Si-29 (p,p')
1.45 + K-40
1.49
500
800
1.97
3.05 (2)
2.27
3.43 (2)
2.81
1100
1300
1600
3.05
4.38 (2)
1800
2200
CHANNEL NO.

FIGURE 24 (A)

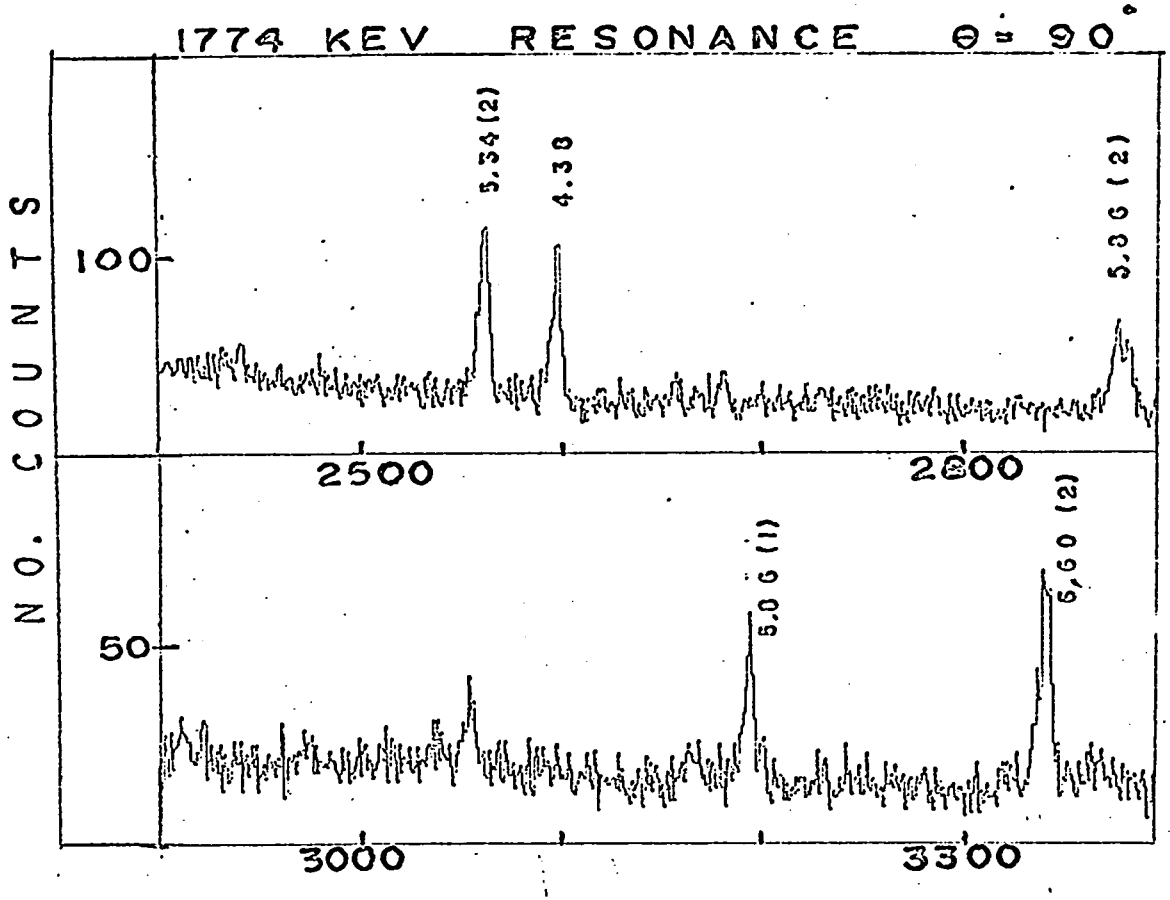
1774 KEV RESONANCE θ = 90°
NO. COUNTS
100
50
5.34 (2)
4.38
5.36 (2)
5.06 (1)
5.60 (2)
2500
2800
3000
3300
CHANNEL NO.

FIGURE 2.4 (B)

The 1.974 Mev gamma-ray displayed a shift of 0.92 ± 0.79 Kev, corresponding to F = .23 ± .20, while the 3.473 Mev line shifted by 8.3 ± 1.7 Kev, corresponding to F = 1.16 ± .24. Finally, the 3.048 Mev gamma-ray, and its second escape peak shifted by 5.4 ± .85 Kev and 6.25 ± 1.7 Kev respectively, corresponding to a mean attenuation coefficient of F = 0.89 ± .13.

As a result of these observations, the lifetime of the 1.974 Mev level was found to be $380\ ^{+3200}_{-220}$ fs, while limits of $\leq$15 fs and $\leq$47 fs were set on the lifetimes of the 4.182 Mev and 4.501 Mev levels respectively.

ii) The Ep = 177.5 Kev Resonance (E_x = 7.313 Mev)

There is evidence, though not conclusive, that this resonance may have a lifetime sufficiently long to give a detectable slowing down of the recoil ion before emission of the first gamma-ray.

The resonance level decays to the 2.936, 1.974 and 1.453 Mev levels, giving gamma-rays of 4.377, 5.339 and 5.860 Mev respectively. The 1.974 Mev level is populated in roughly equal amounts by this resonance and by the Ep = 1773 Kev resonance. If the lifetime of the resonance were very short-lived ($\tau < 10^{-15}$ sec), one would expect a full Doppler shift in the energy of the gamma-rays, i.e., shifts of 9.00 Kev, 11.00 Kev, and 12.07 Kev respectively. It was observed, however, that the 4.377 Mev gamma-ray (and second escape peak) shifted by 8.52 ± .48 Kev and 8.44 ± .47 Kev respectively, which corresponds to $\overline{F}$ = .94 ± .04.

Also, the 5.339 Mev gamma-ray shifted by 10.57 ± .45 Kev, resulting in F = .96 ± .04. The 5.860 Mev gamma-ray (first and second escape peaks) displayed shifts of 11.89 ± .65 Kev and 10.61 ± .72 Kev respectively, leading to values of F = .98 ± .05 and F = .88 ± .06. If one takes the average attenuation coefficient for the decays from resonance to the 2.939 and 1.453 Mev levels, one obtains $\bar{F}$ = .945 ± .03 indicating that the lifetime of the resonance level is 10^{+6}_{-5} fs.

The decay from both the Ep = 1773 Kev and the Ep = 1775 Kev resonances to the 1.974 Mev level yields F = .96 ± .04. The fact that the 1775 Kev resonance level is long-lived would give an attenuated Doppler shift for the decay to the 1.974 Mev level, since the two resonance gamma-rays populating this level are only 2 Kev apart.

The observed Doppler shifts for the 2.936→1.453 Mev and 2.936→0.680 Mev transitions were 1.73 ± .34 Kev and 2.86 ± .88 Kev respectively, giving a mean $\bar{F}$ = .57 ± .10. If it is assumed that the resonance level is very short-lived ($\tau<10^{-15}$ sec), this leads to a lifetime of $\tau = 100^{+45}_{-31}$ fs, However, if the lifetime is corrected for the fact that the resonance level lifetime is τ_1 = 10 fs, this leads to a lifetime for the 2.94 Mev level of $\tau = 85^{+40}_{-30}$ fs. Figure 25 shows the $F(\tau)$ vs τ curve for this resonance. The effect of τ_1 (resonance level) = 10 fs on $F(\tau)$ is also shown on the curve.

Also, if the lifetime of the 1.974 Mev level is corrected for τ_1 = 10 fs, this gives $\tau(1.974) = 340^{+2800}_{-200}$ fs. Thus, the average lifetime for the 1.974 Mev level, calculated from both resonances, is taken to be $\tau = 360^{+3100}_{-220}$ fs.

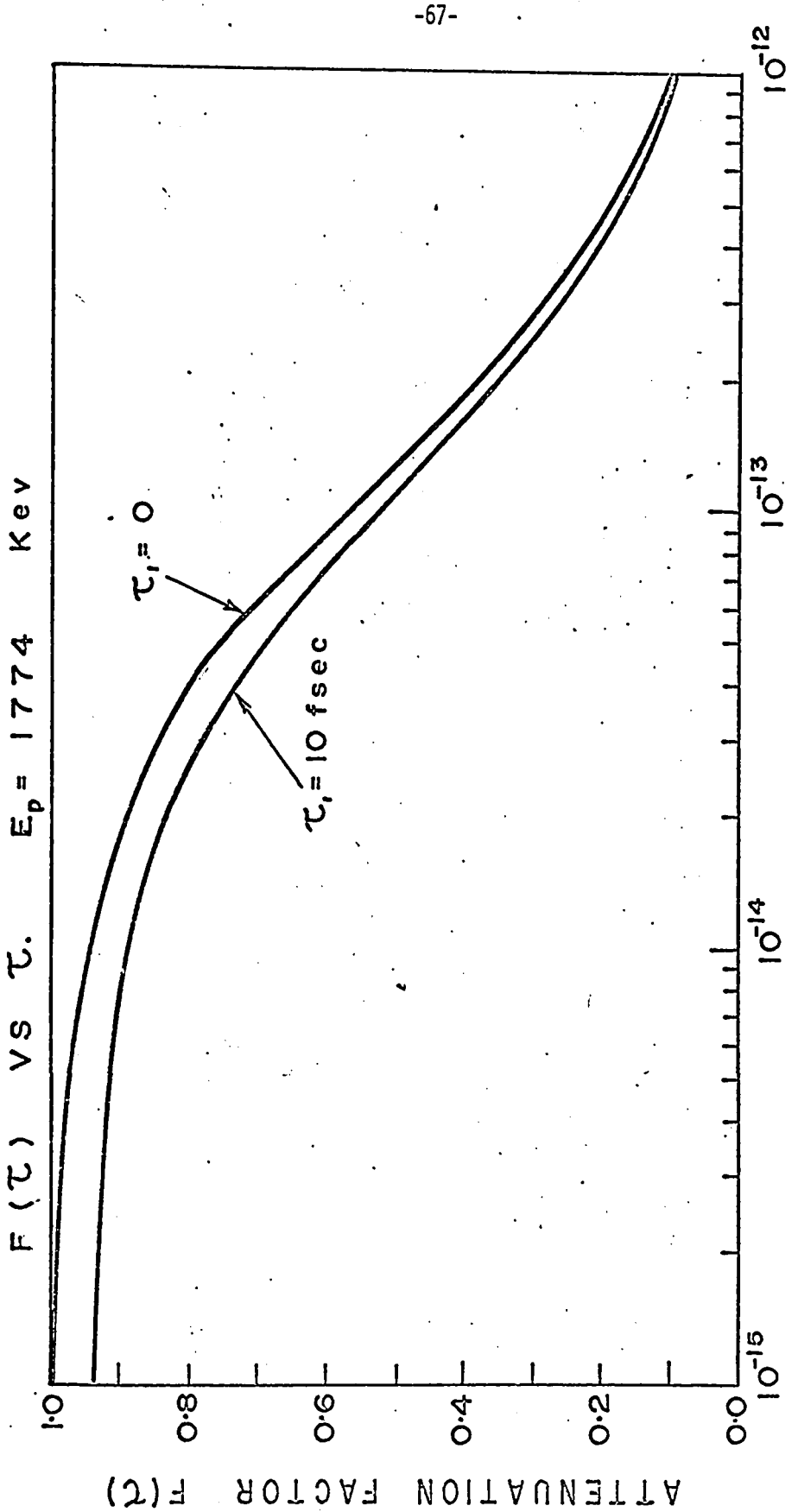
F(τ) VS τ. E_p = 1774 Kev
τ_i = 0
τ_i = 10 fsec
ATTENUATION FACTOR F(τ)
1·0
0·8
0·6
0·4
0·2
0·0
10^{-15}
10^{-14}
10^{-13}
10^{-12}
MEAN LIFETIME (sec)

FIGURE 25

No drifts in gain were discovered in this section of the experiment, as is demonstrated by the fact that the gamma-rays de-exciting the Ep = 1773 Kev resonance were fully Doppler shifted, within experimental errors. Also, the 0.709→0 transition, which is long-lived ($\tau <$ 1100 fs) showed no drift between 0^0 and 90^0. Finally, a ThC" source also showed no change in its centroid at the two angles.

Figure 26 shows the attenuated Doppler shift observed in the 1.486 Mev gamma-ray, resulting from the transition between the 2.939→1.453 Mev levels.

Table 7 summarizes the results obtained from the Ep = 1773-1775 Kev doublet.

In Table 8, the lifetimes of the excited states studied in this paper are compared with those obtained by Harris et al[8] and by Kennedy et al[1].

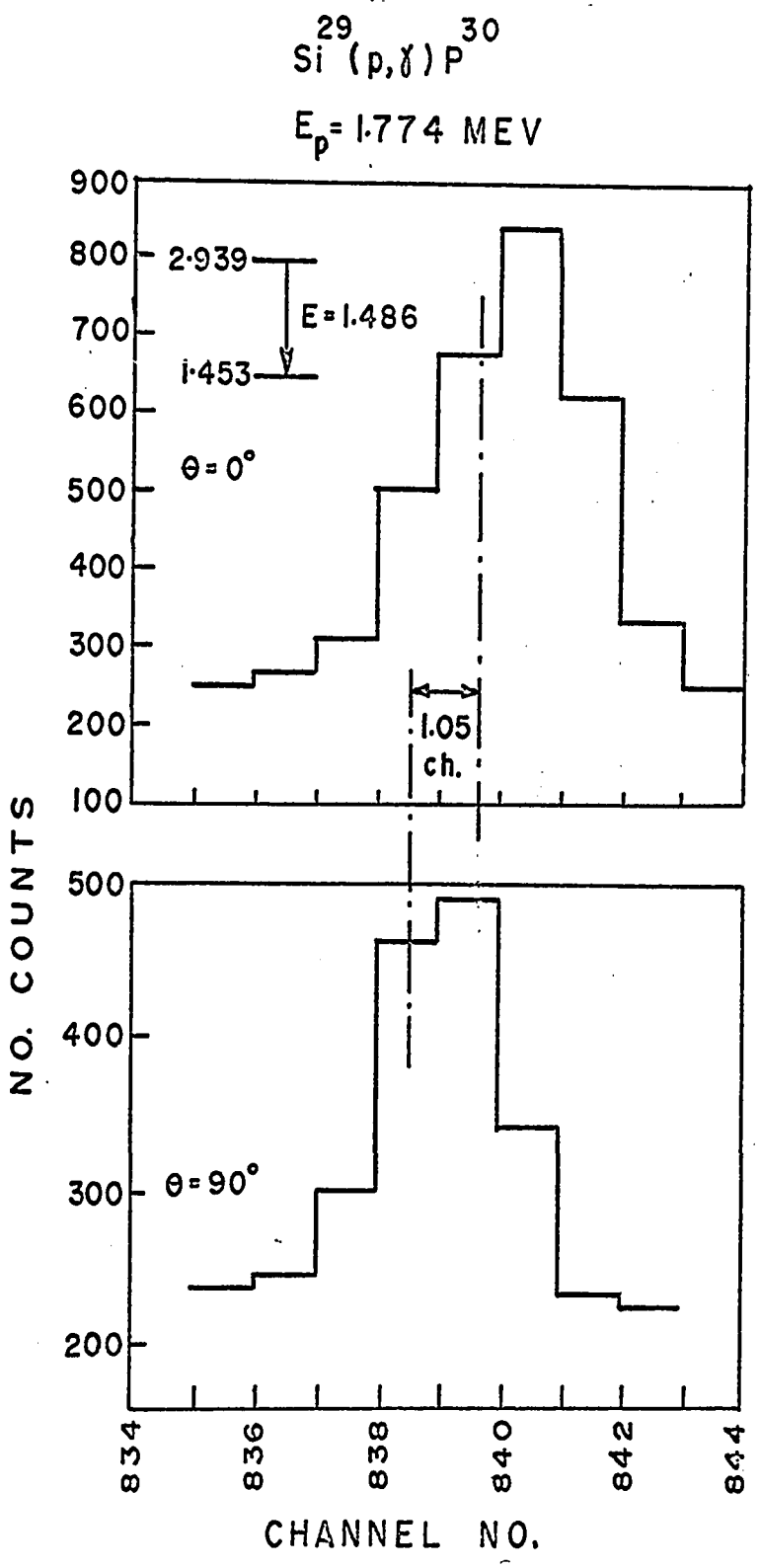
$Si^{29}(p,\gamma)P^{30}$
E_p= 1.774 MEV
2.939
E=1.486
1.453
θ=0°
1.05
ch.
θ=90°
NO. COUNTS
CHANNEL NO.
900
800
700
600
500
400
300
200
100
500
400
300
200
834
836
838
840
842
844

FIGURE 26

TABLE VII-A

Results of the E_p=1773 Kev Resonance.

Transition	E_γ (Mev)	ΔE_γ (Kev)	$(\Delta E_\gamma)_{fds}$ (Kev)	$F(\tau)$ (%)	$\overline{F(\tau)}$ (%)	τ (fsec)
R →.709	6.602 (2)	14.27±.68	13.60	105±5	104±5	full shift
R →4.501	2.810	5.98±.65	5.79	103±11		
R→1.974	5.337 (2)	10.57±.45	11.00	96±4	96±4	
1.974→0	1.974	0.92±.79	4.07	23±20	23±20	360^{+3100}_{-220}
4.182→.709	3.473	8.30±1.70	7.15	116±24	116±24	≤15
4.501→1.45	3.048	5.40±.85	6.28	86±14	89±13	≤47
	3.048 (2)	6.25±1.70	6.28	99±27		

TABLE VII-B

Results of the E_p=1775 Kev Resonance.

Transition	E_γ (Mev)	ΔE_γ (Kev)	$(\Delta E_\gamma)_{fds}$ (Kev)	$F(\tau)$ (%)	$F(\tau)$ (%)	τ (fsec)
R→1.453	5.860	11.89±.65	12.07	99±5		
	5.860 (2)	10.61±.72	12.07	88±6	94±3	10^{+6}_{-5}
R→2.939	4.377	8.52±.48	9.00	95±4		
	4.377 (2)	8.44±.47	9.00	94±4		
R→1.974	5.339 (2)	10.57±.45	11.00	96±4	96±4	
1.974→0	1.974	0.92±.79	4.07	23±20	23±20	360^{+3100}_{-220}
2.939→1.453	1.486	1.73±.34	3.06	56±11	57±10	85^{+40}_{-30}
2.939→0.678	2.261	2.86±.88	4.66	61±19		

TABLE VIII

Comparison of Doppler Shift Lifetimes in P^{30}

E_p (Kev)	Transition Initial (Mev)	Transition Final (Mev)	$F(\tau)$ Present (%)	τ Present (fsec)	τ Harris[8] (fsec)	τ Kennedy[1] (fsec)
1505	4.231	1.974	5±3	2000^{+3000}_{-800}	≥1200	
	4.624	1.453	34±9	215^{+105}_{-65}	260±60	
1643	3.020	0.678	103±11	≤14		
	0.709	0.000	4±5	≥1100		≥3000
1686	4.142	0.000	80±3	38±7	58±14	
1773	1.974	0.000	23±20	360^{+3100}_{-220}	≥240	
	4.182	0.709	116±24	≤15		
	4.501	1.453	89±13	≤47		
1775	7.313	1.453	94±3	10^{+6}_{-5}		
	7.313	2.939				
	2.939	1.453	57±10	85^{+40}_{-30}	37±5	
	2.939	0.678				

CHAPTER 4

CONCLUSION

A Lithium-drifted Germanium spectrometer has proved a useful tool to determine some lifetimes in P^{30} via the $Si^{29}(p,\gamma)P^{30}$ reaction. It has been shown that, if the stopping power for the combination of recoil ion and stopping medium is known, a measurement of the energy of a given gamma-ray, emitted from a nucleus which is slowing down in a solid, as a function of angle, will yield the lifetime of an excited level if this lifetime is in the range 10^{-12} sec. to 10^{-14} sec. The Doppler shift attenuation coefficient, $F(\tau)$, which is determined experimentally for a given gamma-ray, has been related to the lifetime of the level which emits the gamma-ray.

Since the shifts in energy due to the Doppler effect were small in these proton capture reactions, $\left(\frac{\Delta E_\gamma}{E_\gamma}\right)_{F.D.S.} \simeq .2\%$ it was important to have a Ge(Li) spectrometer system which was stable over the experimental runs. The system which was utilized was found to be stable to within .5 channels during an elapsed time of 78 hours.

It was found that the main source of experimental error was not due to gain drifts in the electronic system, but rather to the statistical uncertainties in the peak centroids, caused by background radiation. In future experiments, it would prove advantageous to try to reduce this background by, for example, shielding the detector, or by reducing

the amount of contaminants in the target region. By far the greatest source of error in the Doppler shift method arises from the uncertainty in the stopping power, especially at the low recoil energies used in these experiments. Since there was no experimental data on the stopping of P^{30} ions by $Si^{29}O_2$, it was necessary to use the theory developed by Lindhard et al., which has an uncertainty of about 20%.

As a result of the measurements described in this thesis, it was found that the lifetimes of the 1.974, 2.939, 4.142, 4.231, and 4.624 Mev levels were 360^{+3100}_{-215} fs, 85^{+41}_{-28} fs, 38 ± 7 fs, 2000^{+3000}_{-800} fs, and 212^{+105}_{-62} fs, respectively. Limits were set on the lifetimes of the following levels 0.709 ($\geq$1100 fs), 3.020 ($\leq$14 fs), 4.182 ($\leq$15 fs) and 4.501 Mev ($\leq$47 fs).

There is also evidence that the lifetime of the Ep = 1775 Kev resonance level (Ex = 7.313 Mev) is sufficiently long to give a detectable slowing down in the velocity of the recoil ion before emission of the first gamma-ray. The average Doppler shift attenuation coefficient for this resonance level was found to be $\overline{F} = .94 \pm .03$, leading to a lifetime of 10^{+6}_{-5} fs.

The strength of this resonance $S = (2J + 1)\Gamma_p\Gamma_\gamma/\Gamma$ is given as 1.1 ± .2 ev by Harris et al[8], who favour J = 3 from the results of their correlation measurements. This strength sets an upper limit of 1.3 fs for the lifetime, which would occur when $\Gamma_p = \Gamma_\gamma = 1/2\Gamma$. Such a lifetime is too short to detect by Doppler shift methods and is inconsistent with the above interpretation. A possible explanation is that the transition to the 2.94 Mev and 1.453 Mev levels may not be entirely from the 1775 Kev member of the resonance doublet.

A slight difference in the angular distributions of the two gamma-rays which differ in energy by 2 Kev could give a centroid shift different from that expected for the full Doppler shift of a single gamma-ray energy.

REFERENCES

1. E. F. Kennedy, D. H. Youngblood, A. E. Blaugrund.
Physical Review 158, 897 (1967)

2. R. A. Moore
Thesis, University of Kansas, 1963 (unpublished)

3. A. K. Val'ter, E. G. Kopanets, A. N. L'vow, S.P.T. Tsytko.
Izv. Akad. Nauk SSSR, Ser. Fiz. 27, 242 (1963)

4. P. A. Phelps, E. A. Milne, H. E. Handler.
Physical Review 138, B1088 (1965)

5. P. M. Endt, C. van der Leun.
Nuclear Physics A105 , 1 (1967)

6. G. I Harris, A. K. Hyder Jr.
Physical Review 157, 958 (1967)

7. C. W. Vermette, W. C. Olser, D. A. Hutcheon, D. H. Sykes.
Nuclear Physics A111, 39 (1968)

8. G. I. Harris, A. K. Hyder Jr., J. Walinga
Physical Review 187, 1413 (1969)

9. S. Devons, G. Manning, D. Bunbury
Proc. Phys. Soc. A68, 18 (1955)

10. R. Gauthier

University of Ottawa (private communication)

11. H. E. Schiott

Matematisk - fysiske Meddelelser 35, no. 9 (1966)

12. L. C. Northcliffe

Ann. Rev. Nucl. Sci. 13, 67 (1963)

13. J. Lindhard, M. Scharff, H. E. Schiott.

Mat. Fys. Medd. Dan. Vid. Selsk. 33, no. 14 (1963)

14. A. E. Blaugrund

Nuclear Physics 88, 501 (1966)

15. J. H. Ormrod, H. E. Duckworth

Canadian Journal of Physics 41, 1424 (1963)

J. H. Ormrod, J. R. MacDonald, H. E. Duckworth

Canadian Journal of Physics 43, 275 (1965)

16. G. A. P. Engelbertink, H. Linderman, M. J. N. Jacobs

Nuclear Physics A107, 305 (1968)

APPENDIX

Stopping Power Considerations

The Doppler shift attenuation coefficient is

$$F(\tau) = \frac{1}{(\tau_1 - \tau)v(o)} \int_o^\infty \left[\exp\left(-\frac{t}{\tau_1}\right) - \exp\left(-\frac{t}{\tau}\right)\right] \overline{v(t)} \; \overline{\cos\phi(t)} \; dt \quad \ldots\ldots (30)$$

To calculate $F(\tau)$, one must therefore know the velocity function, $\overline{v(t)}$, and the mean scattering angle, $\overline{\cos\phi(t)}$. Blaugrund[14] uses dimensionless variables to calculate $F(\tau)$.

$$\varepsilon = \frac{a A_2}{Z_1 Z_2 e^2 (A_1 + A_2)} E \quad \ldots\ldots (31)$$

where $a = a_0 \times .8853 \left[Z_1^{2/3} + Z_2^{2/3} \right]^{-1/2} (cm)$

a_0 = Bohr radius = $\frac{\hbar^2}{me^2}$

e = electronic charge (e.s.u.)

Z = atomic number

A = mass number

E = energy of the recoil ion (ergs)

Subscript 1 refers to the recoiling ion

Subscript 2 refers to the stopping medium.

In these experiments, the value of ε corresponding to an initial recoil velocity of $\frac{v(o)}{c} = .2\%$ is $\varepsilon_o = .85$.

$$\rho = \frac{4\pi a^2 N A_1 A_2}{(A_1 + A_2)^2} \quad x \qquad \text{..... (32)}$$

where N = number of scattering atoms per unit volume (# atoms/cc)

x = distance (cm)

For velocities $V < \frac{c}{137} Z_1^{2/3}$, the electronic stopping power is, to a good approximation, given by

$$\left(\frac{d\varepsilon}{d\rho}\right)_e = k \varepsilon^{1/2} \qquad \text{..... (33)}$$

where $$k = \xi X \frac{.0793 Z_1^{1/2} Z_2^{1/2} (A_1 + A_2)^{3/2}}{(Z_1^{2/3} + Z_2^{2/3})^{3/4} A_1^{3/2} A_2^{1/2}} \qquad \text{..... (34)}$$

(= .224 in our case)

and ξ is a constant which Lindhard, Scharff and Schiott[13] assume to be $\xi = Z_1^{1/6}$.

Experimentally, it was found by Ormrod et al. that

$\left(\frac{d\varepsilon}{d\rho}\right)_e = k\varepsilon^p$, where $.4 \leq p \leq .6$.

For the atomic stopping power, Lindhard et al. arrived at a universal differential atomic scattering cross-section

$$d\sigma(\theta) = \frac{\pi a^2 dt}{2\, t^{3/2}}\, f(t^{1/2}) \qquad \ldots\ldots\ldots\ldots\ldots (35)$$

where $t^{\frac{1}{2}} = \varepsilon \sin \frac{1}{2}\theta$

and θ = deflection angle in the center of mass system

The function $f(t^{\frac{1}{2}})$ is given in figure 1 of Lindhard's article.

The atomic stopping power is then taken to be

$$\left(\frac{d\varepsilon}{d\rho}\right)_a = \frac{1}{\varepsilon}\int_0^{\varepsilon} f(x)\, dx \qquad \ldots\ldots\ldots\ldots\ldots (36)$$

Engelbertink et al[16] have fitted the curve given as figure 1 in Lindhard's article with the function

$$\left(\frac{d\varepsilon}{d\rho}\right)_a = -0.2 \log_{10}\left[\frac{\varepsilon^{1.215}}{70} + \frac{.002}{\varepsilon^{.815}}\right] \qquad \ldots\ldots\ldots\ldots (37)$$

This function, along with Lindhard's curve is given in figure 15.

The total stopping power is the sum of the electronic and atomic contributions, i.e.,

$$\left(\frac{d\varepsilon}{d\rho}\right) = \left(\frac{d\varepsilon}{d\rho}\right)_a + \left(\frac{d\varepsilon}{d\rho}\right)_e$$

Figure 16 gives a comparison between $(\frac{d\varepsilon}{d\rho})_a$ and $(\frac{d\varepsilon}{d\rho})_e$, calculated from a value of k = .224.

Blaugrund calculates the mean cosine of the scattering angle as

$$\overline{\cos\phi} = \exp\left[-\frac{1}{2}\frac{A_2}{A_1} G(r)\ I\right] \quad \text{..... (38)}$$

where
$$G(r) \doteq 1 + \frac{2}{3}r - \frac{7}{15}r^2 \quad \text{for } r<1$$
$$\doteq \frac{2}{3} + \frac{8}{15}r \quad \text{for } r<1 \quad \text{..... (39)}$$

where $$r = \frac{A_1}{A_2}$$

and
$$I = \int_{\varepsilon}^{\varepsilon_0} \frac{(d\varepsilon/d\rho)_a}{(d\varepsilon/d\rho)}\, d\varepsilon \quad \text{..... (40)}$$

and $$\left(\frac{d\varepsilon}{d\rho}\right) = \left(\frac{d\varepsilon}{d\rho}\right)_a + \left(\frac{d\varepsilon}{d\rho}\right)_e$$

Also, the following additional dimensionless variables are used:

$$T = \frac{\hbar}{e^2}\frac{(A_1 + A_2)^2}{4\pi a^2 N A_1 A_2} \quad \text{.....(41)}$$

$$\nu = \frac{(\hbar c)}{e^2}\left(\frac{v}{c}\right) \quad \text{where v = velocity ..... (42)}$$

The following relation defines the variable M

$$\varepsilon = \frac{1}{2} M\nu^2 \qquad \text{..... (43)}$$

From the equation 31 and the definition of ν (equation 42), it follows that

$$M = \frac{1.63 \times 10^3 A_1 A_2}{Z_1 Z_2 (Z_1^{2/3} + Z_2^{2/3})^{1/2} (A_1 + A_2)} \qquad \text{..... (44)}$$

The number 1.63×10^3 is the product of .8853 times the ratio of the proton mass to the electron mass.

Dimensionless time is taken as $\theta = \frac{t}{T}$, such that $\frac{d\rho}{d\theta} = \nu$.

Since $\varepsilon = \frac{1}{2} M\nu^2 = \frac{1}{2} M \left(\frac{d\rho}{d\theta}\right)^2$, then

$$(d\theta)^2 = \frac{M}{2\varepsilon} (d\rho)^2$$

and $$d\rho = \left(\frac{2\varepsilon}{M}\right)^{1/2} d\theta$$

$$\left(\frac{d\rho}{d\varepsilon}\right) d\varepsilon = \left(\frac{2\varepsilon}{M}\right)^{1/2} d\theta$$

$$\therefore d\theta = \left(\frac{M}{2\varepsilon}\right)^{1/2} \frac{d\varepsilon}{(d\varepsilon/\theta\rho)}$$

and $$\theta = \left(\frac{M}{2}\right)^{1/2} \int_{\varepsilon}^{\varepsilon_0} \frac{d\varepsilon}{\varepsilon^{\frac{1}{2}} [\, d\varepsilon/d\rho]} \qquad \text{.....(45)}$$

In dimensionless variables, the attenuation coefficient, $F(\tau)$, becomes

$$F(\tau) = \left(\frac{M}{2}\right)^{1/2} \frac{T}{(\tau_1 - \tau)\,\varepsilon_0^{1/2}} \int_{\varepsilon_0}^{0} \frac{\left[\exp\left(-\frac{\theta T}{\tau_1}\right) - \exp\left(-\frac{\theta T}{\tau}\right)\right] \overline{\cos\phi}\, d\varepsilon}{d\varepsilon / d\rho} \qquad \text{.....(46)}$$

The above equations hold for a stopping medium containing only one type of atom. If the medium contains several types of atoms, let M, Z_2, A_2 etc. refer to the heaviest of these atoms, and let M_i, Z_{2i}, A_{2i}, etc. refer to the i^{th} type of lighter atom.

Therefore,

$$\theta = \left(\frac{M}{2}\right)^{1/2} \int_{\varepsilon}^{\varepsilon_0} \frac{d\varepsilon}{\varepsilon^{1/2}\left[\left(\frac{d\varepsilon}{d\rho}\right) + \Sigma Ci \left(\frac{d\varepsilon}{d\rho}\right)_i\right]} \qquad \text{.....(47)}$$

where θ and ε refer to the heaviest scattering atom and

$$C_i = \frac{Ni}{N} \frac{Z_{2i}}{Z_2} \frac{a_i}{a} \frac{A_1 + A_2}{A_1 + A_{2i}} \qquad \text{.....(48)}$$

and $\left(\frac{d\varepsilon}{d\rho}\right)_i$ is the total specific energy loss calculated at the energy $\left(\frac{Mi}{M}\right)\varepsilon$.

In a similar way, $\overline{\cos\phi}$ can be calculated from equations 38, 39, 40 by using

$$I = \int_{\varepsilon}^{\varepsilon_0} \frac{(d\varepsilon/d\rho)a + \Sigma Ci\ (A_{2i}/A_2)(Gi/G)\ (d\varepsilon/d\rho)a_i}{\varepsilon\ [(d\varepsilon/d\rho) + \Sigma Ci\ (d\varepsilon/d\rho)_i]}\ d\varepsilon \quad .....(49)$$

Thus, the general equation for the Doppler shift attenuation coefficient is

$$F(\tau) = \left(\frac{M}{2}\right)^{1/2} \frac{T}{(\tau_1 - \tau)\sqrt{\varepsilon_o}} \int_{\varepsilon_o}^{o} \frac{[\exp(-\theta T/\tau_1) - \exp(-\theta T/\tau)]\ \overline{\cos\phi}}{\left[\left(\frac{d\varepsilon}{d\rho}\right) + \sum_i C_i \left(\frac{d\varepsilon}{d\rho}\right)_i\right]}\ d\varepsilon$$

.....(50)